STATISTICAL ANALYSIS OF INDOOR UWB CHANNEL PARAMETERS IN DIFFERENT WALL CORRIDORS AND THROUGH-WALL ENVIRONMENTS

by

SREEVINAY NETRAPALA

Presented to the Faculty of the Graduate School of

The University of Texas at Arlington in Partial Fulfillment

of the Requirements

for the Degree of

MASTER OF SCIENCE IN ELECTRICAL ENGINEERING

THE UNIVERSITY OF TEXAS AT ARLINGTON

August 2015

Acknowledgements

In an endeavor to successfully complete my thesis, I received assistance from many people and I take this opportunity to thank those who have helped me along the way to achieve this success.

I am grateful to my research advisor, Dr. Qilian Liang for his guidance and continuous support throughout my thesis. His patience and knowledge have been invaluable throughout my research and I express my deep sense of gratitude to him. I would like to thank Dr. Alan Davis and Dr. William Dillon for taking time to be on my thesis committee. I would like to thank my lab mates Shruthishree B.K, Roopesh Kumar and Karishma Katara for their valuable suggestions and support to collect data during the course of my thesis.

I am indebted to my parents and my brother for always encouraging me and standing by my side. I would like to thank all my friends for their support and encouragement.

July 2, 2015

Abstract

STATISTICAL ANALYSIS OF INDOOR UWB CHANNEL PARAMETERS IN DIFFERENT WALL CORRIDORS AND THROUGH-WALL ENVIRONMENTS

Sreevinay Netrapala, M.S.

The University of Texas at Arlington, 2015

Supervising Professor: Qilian Liang

The indoor channel parameters appears different for Ultra Wide Band (UWB) systems than it does to narrow band systems. Generally UWB pulses are short and do not overlap in time like multipath sine waves. According to electromagnetic theory, lower frequencies have better penetrating properties. The combination of larger spectrum and lower frequencies possessed by UWB signals makes it easy to penetrate through walls, floors, doors, wood, ceilings, etc. This penetration property plays a very important role in indoor UWB communication system. This thesis presents the statistical analysis of large scale, small scale and time dispersal parameters in different wall corridor environments and through-the-walls (Gypsum wall) in indoor classroom environments.

Channel modeling usually includes the characterization of different channel parameters like path loss, shadowing, multipath delay spread, and coherence bandwidth, multipath arrival times, average multipath intensity profile, received amplitude distribution of the multipath components. Different UWB channel models exists for indoor environment in literature. In this thesis, the Channel Impulse Response (CIR) of the environments are extracted from the CLEAN algorithm and with this CIRs and also able to extract other small scale and time dispersal channel parameters. The large scale parameters were also

extracted and the path loss exponent was compared with different indoor environments. From the power decay profile, RMS delay, mean excess delay, and average RMS values were calculated. The variations in the parameter values and the distribution fits were analyzed and noted to better estimate the channel.

The experiments were solely conducted in classroom 202-203 and corridors in Nedderman Hall, 2nd and 3rd floor at the University of Texas at Arlington. The experimental results have been discussed.

Table of Contents

List of Illustrations

List of Tables

Chapter 1

INTRODUCTION

1.1 Motivation

The propagation of UWB signals in indoor environments is an important issue with significant impacts on the future direction and scope of the UWB technology and its applications. The objective of this work is to obtain a better assessment of the potentials of UWB indoor communications by characterizing the UWB indoor communication channel. Channel characterization refers to extracting the channel parameters from measured data. An indoor UWB measurement campaign is undertaken and time-domain indoor propagation measurements using a pulse width of 61 pico-seconds (ps) are carried out. Typical indoor scenarios, including Line-Of-Sight (LOS), Non-Line-Of-Sight (NLOS), room-to-room, through the wall, within the-room, and hallways, are considered. Results for indoor propagation measurements are presented for small-scale fading parameters, large scale fading parameters and time dispersal parameters. The statistical analysis and simulation results of the path-loss exponent (n), time dispersion parameters, and through the wall channel modeling (Classroom environment) are presented.

The primary hardware used for this study is PulsON 410 developed by the Time Domain Corporation. The focus of this thesis report is on *through the wall channel modeling* and *variation of path loss exponent values in different types of indoor environments,* using PulsON 410 UWB radar in Bistatic mode. The few major advantages of using the PulsON 410 technology can be listed as:

- Extremely low power
- Spectral efficiency
- Immunity to interference

- Excellent wall penetration characteristics
- Easy for conducting experiments

This radar also supports different types of software from Time Domain Inc. which plays a major role in conducting experiments.

1.2 Thesis Organization

Chapter 2 presents background information about UWB technology along with some regulatory issues. Chapter 3 Indoor Channel modeling, modeling techniques, and modeling parameters like small scale, large scale, time dispersal parameters and path loss exponent (n). Chapter 4 discusses the UWB test equipment, the setup and tests conducted. A detailed analysis of the test results for different environment scenarios are provided in Chapter 5. Chapter 6 offers conclusions and recommendations for future research.

Chapter 2

BACKGROUND

This chapter gives an introduction of the Ultra-Wideband (UWB) technology and the channel characterization fundamentals. First a global overview of the UWB technology is presented. The important definitions and equations for channel characterization and a brief description of different channel sounding techniques are introduced in further chapters.

2.1 Ultra-Wideband Technology Overview

UWB technology is currently developing very fast and attracts more and more global attention. The term “Ultra-Wideband” refers to the spectral characteristics of this technology. It also has been called impulse radio, carrier less radio or carrier-free radio in the early days. UWB technology uses the radio spectrum differently than the vast majority of radio communication technologies. First, the bandwidth of UWB systems is much greater than the bandwidth of any current wideband wireless system. The FCC defines an UWB transmitter as an intentional radiator for which the -10dB bandwidth is equal to or greater than 20% of the center frequency or the –10 dB bandwidth is at least 500 MHz. Second, unlike conventional wireless systems that use radio frequency (RF) carriers, many UWB applications such as radar-ranging systems and imaging systems usually do not use RF carriers. Instead, they use short impulses that have extremely fast rise and fall times in the sub-nanosecond range and in the frequency domain these signals occupy large frequency range from near-DC to several GHz.

The formula proposed by the FCC commission for calculating the fractional bandwidth is [3]

$$FractionalBandwidth = \frac{f_H - f_L}{\frac{f_H + f_L}{2}} \quad (2.1)$$

where f_H represents the upper frequency of the -10 dB emission limit and

f_L represents the lower frequency limit of the -10dB emission limit.

UWB is based on the generation of very short duration pulses of the order of picoseconds. The information of each bit in the binary sequence is transferred using one or more pulses by code repetition. This use a number of pulses increases the robustness in the transmission of each bit. In UWB communications there is no carrier used and hence all the references are made with respect to the center frequency (f_c) [4].

$$CenterFrequency(f_c) = \frac{f_H + f_L}{2} \quad (2.2)$$

In Ultra wideband communications, a signal with a much larger bandwidth is transmitted with a low power spectral density. This approach has a potential to produce signal which has higher immunity to interference effects and good time of arrival resolution. UWB communications employ the technique of impulse radio. Impulse radio communicates with the help of base band pulses of very short duration of the order of nanoseconds, thereby spreading the energy of the signal from dc to a few gigahertz. The fact that the impulse radio system operates in the lowest possible frequency band that supports its wide transmission bandwidth means that this radio has the best chance of penetrating objects which become opaque at higher frequencies.

Impulse radios operating in the highly populated frequency range below a few gigahertz must contend with a variety of interfering signals. They must also guarantee that they do not interfere with the narrow-band radio systems operating in dedicated bands. These requirements necessitate the use of spread spectrum techniques. A means of

spreading the spectrum of the ultra-wideband pulses is to employ time hopping with data modulation accomplished by additional pulse position modulation at the rate of many pulses per data symbol. The use of signals with gigahertz bandwidth means that multipath is resolvable down to path differential delays on the order of nanoseconds or less i.e. down to path length differentials on the order of a foot or less. This significantly reduces fading effects even in indoor environments. The advantages of UWB over conventional narrowband systems are [3]:

- Large Instantaneous bandwidth that enables fine time resolution for network time distribution, precision location capability, or use as a radar.
- Short duration pulses that provide robust performance in dense multipath environments by exploiting more resolvable paths.
- Low power spectral density that allows coexistence with existing users and has a
- Low Probability of Intercept (LPI).
- Data rate may be traded for power spectral density and multipath performance.

Chapter 3

INDOOR CHANNEL MODELING

3.1 Introduction

The measurement and modeling of UWB channels is a fairly recent field. The 802.15 channel model is based on some of the measurement campaigns published in the open literature see, e.g., [2], as well as on measurement campaigns performed explicitly for the standard. These new campaigns were carried out by various standardization participants, and their data were used to assess the efficiency of various proposed channel models, as well as to calibrate their parameters. There are two basic techniques for UWB channel sounding.

1. In time-domain techniques, the channel is excited by a short pulse, and the receiver records the impulse response directly, by sampling the received waveform. The advantage of this technique is that it gives the waveform directly in the time domain, and time variations of the channels can be easily measured. The drawback lies in the problems of producing ultra-short pulses, and the fact that a non-ideal transmit pulse distorts the observed impulse response. Applying a deconvolution of the transmit pulse from the received signal often leads to numerical problems.

2. In swept-frequency measurements, a chirp (time varying sinusoid) is used to excite the channel, so that the received signal is an approximation of the transfer function. In most practical cases, a network analyzer is used a transceiver, since these devices are well-calibrated, and readily available in most laboratories [2]. A further advantage of this technique is that a “back-to-back calibration” can be done quite easily. A drawback is that time variations of the channels cannot be easily recorded. However, this was not a major requirement for the modeling in the 802.15 standard. All the measurement environments

were indoor, since this is the target application for 802.15.3a devices. Different types of indoor environments were analyzed, including residential (homes, apartments), and office environments. The building materials and geometrical layouts are quite different in those cases, and result in distinct channel characteristics. This is due mostly to the higher proportion of metal construction materials found in office buildings as compared to residential buildings. In addition to these environment types, most contributors distinguished between line-of-sight channels, in which there is an unobstructed path from transmitter to receiver, from non-line-of-sight channels. Also, the choice of measurement points were different: some campaigns used regular grids in order to isolate small-scale from large-scale fading effects, while other campaigns used only random placement of measurement points on a large scale. The amount of measurement results was actually too large for an efficient application to the modeling process. The 802.15.3a channel modeling subgroup thus selected a subset of measurements that was to be used for the actual parameterization of measurements, as well as the goodness-of-fit test of those models. Part of these measurements has been made publicly available at [2].

3.2 Statistical Modeling

In statistical channel modeling, measurements are typically conducted to obtain information about the channel in the environment in which we are interested. The data collected from the measurements is then processed to obtain the channel parameters. The statistical information about the channel obtained from these models is often accurate and since the complexity of the environment is not a matter of concern while taking measurements; it is obviously easier to statistically model channels.

3.3 Multipath Fading

A signal travelling from the transmitter to the receiver through a channel usually experiences the three basic propagation mechanisms i.e. reflection, diffraction and scattering due to various objects present in the environment [3]. Multiple components of the signal are formed and these components which arrive at the receiver from many directions are combined to obtain the resultant signal. If the transmitter or the receiver is in motion, the components arrive with varying path lengths, time delays and phases.

Depending upon the phase of the components, they are added constructively or destructively to form the resultant signal. This phenomena leads to distortion and fading of the received signal.

3.4 Large Scale Fading

Large scale modeling involves modeling the signal attenuation with distance. This large scale attenuation is generally referred to as path loss. Path loss is a fundamental characteristics of electromagnetic waves and is incorporated in the system design, via link budgets, to predict expected received power [3].

3.4.1 Path Loss Model

We define path loss as the dB reduction in power from the transmitter to the receiver location, where the received power is spatially averaged around the location. Specifically it is averaged over an area whose radius is several wavelengths, with the wavelength being that at the center frequency of the transmission. A general path loss formula that incorporates reflection, diffraction and scattering for both LOS and NLOS paths can be stated. It has the well-known form [5]

$$PL(d) = PL_0 + 10 * n * \log_{10}(d / d_0) + S \quad (3.5)$$

where, is the point at the reference distance

and n is the slope of the average increase in path loss with dB distance.

The variation S denotes a zero-mean Gaussian random variable with standard deviation s. It can thus be written as,

S = y*s

Where, y is a zero-mean, unit-variance Gaussian random variable. The random variable S is usually referred to as shadowing, and it captures the path loss deviation from its median value.

In the experiments conducted two different scenarios to find the path loss exponent i.e. 'n' in (3.5) for different indoor environments. The statistical analysis helped to conclude that the UWB signal strength vs distance, varies accordingly with the environment. Next section gives us more details about the experiment and conclusions we made.

The above results furthered our interests to move towards the topic "Through the Wall Channel Modeling of UWB signals". The Large scale characteristic analysis are presented in the next section with statistical results.

3.5 Small Scale Fading

In the previous section we concentrated on statistical channel modeling of large scale characteristics of UWB received signals in an indoor environment. This is primarily concerned with the loss in received signal power versus distance between the transmitter and receiver. It was noted that even when modeling relatively simple signal parameters, UWB presents some interesting challenges, and care must be taken when applying a model to a UWB system. We now turn to a more complex part of channel modeling the statistical modeling of the small scale characteristics. The small scale characteristics

include the small scale fading in a local environment as well as the distortion of the transmitted waveform due to multipath. UWB signals are often proposed for short-range applications (d<10m). As a result, when discussing fading (that is, the loss in received signal power) there is some ambiguity in the definition of the large-scale and small-scale. In this section when we discuss signal fading we will typically restrict the term small-scale to refer to fading within a few meter square distance. Large scale fading refers to fading over distance much greater than 1 meter.

3.6 The CLEAN Algorithm

In obtaining a UWB channel model, often the first step is to extract the channel impulse response (CIR) from individual measurements. The CLEAN algorithm introduced is well established in the radio astronomy and microwave communities, is often applied to UWB measurements. The CLEAN algorithm is often preferred because of its ability to produce a discreet CIR in time. In other words, it assumes the channel is a series of impulse, consistent with the tapped-delay line channel model.

To extract CIR from measurements of the received waveform, first we need to consider an LOS measurement to obtain the template for the CLEAN algorithm. The algorithm searches the received waveform iteratively with the template to find the maximum correlation. The steps involved are:

- Calculate the autocorrelation of the template and the cross-correlation of the template with the received waveform.
- Find the largest correlation peak in, record the normalized amplitudes and the relative time delay of the correlation peak.
- Subtract scaled by from at the time delay.

- If a stopping criterion (a minimum threshold on the peak correlation) is not met, go the step 2. Otherwise, stop.

3.7 Channel Impulse Response Approach to Model

The channel impulse response (CIR) is the response obtained at the output of the channel when the input is a unit impulse signal. The CIR can be measured by transmitting a pulse electromagnetic wave over the channel. A radio propagation channel can be considered to be a linearly time varying as well as a spatially varying filter which can lead to distortion of the transmitted signal. The signal that reaches the receiver is typically a number of multipath components which have reduced signal strength, varying time delays and phase shifts. Thus the impulse response of a multipath radio channel is given by

$$h(t,\tau) = \sum_{i=0}^{L-1} z_i(t) a_i(t) \exp[j(2\pi f_c \tau_i(t) + \upsilon_i(t,\tau))] \delta(\tau - \tau_i(t)) \qquad (3.6)$$

where $z_i(t)$ is the persistence process that denotes the presence or absence of a multipath component, $a_i(t)$ represents the amplitude of the multipath component (MPC) at time t, δ(·) is the Dirac delta function, L is the total number of multipath components and is the corresponding excess delay of the MPC. The excess delay is the difference between the arrival times of the last multipath component and the first component. These components are also subjected to phase shifts as they propagate through free space and other phase shifts as they traverse through the channel, and the phase shift is expressed by

$$\exp[j(2\pi f_c \tau_i(t) + \upsilon_i(t,\tau))]$$

In this model, a profile of the impulse response is obtained for each time t and the delay axis τ is divided equally into bins with width. Many multipath components can be received within a particular bin and since these components cannot be resolved or separated, they are added and are all represented by only one multipath component. The addition of a large number of multipath components results in the fading of the signal. If the system is considered to be time invariant, the channel impulse response would be,

$$h(\tau) = \sum_{i=0}^{L-1} z_i a_i \exp[j(2\pi f_c \tau_i + \upsilon_i(\tau)]\delta(\tau - \tau_i)$$

3.8 CIR Parameters

This section discusses the concept of power delay profile and some of the parameters that can be extracted from it. These parameters are often used for representing a channel's delay domain characteristics.

3.8.1 Power Delay Profile

A power delay profile (PDP) is a "power version" of the channel impulse response. A PDP is a plot of the received power versus time delay corresponding to each multipath component. An average PDP is obtained by determining the average of instantaneous power delay profiles measured in a particular area.

Important channel parameters can be obtained from a power delay profile. The channel parameters that are often used to represent a multipath channel are: mean excess delay, root mean square delay spread and maximum excess delay.

3.8.2 Mean Excess Delay

The mean excess delay is the weighted average of the power delay profile. It is the first moment of a PDP and is given by

$$\bar{\tau} = \frac{\sum_i a_i^2 \tau_i}{\sum_i a_i^2}$$

Where a_i^2 is the square of the amplitudes of the MPC and τ_i is the delay.

3.8.3 Root Mean Square Delay Spread (RMSDS)

RMSDS is the square root of the second central moment of a PDP and is given by,

$$RMSD = \sqrt{\bar{\tau^2} - \bar{\tau}^2}$$

Where $$\bar{\tau^2} = \frac{\sum_i a_i^2 \tau^2{}_i}{\sum_i a_i^2}$$

RMSDS is a measure of the multipath spread and it can be used to judge the performance of a communication system. It directly relates to inter-symbol interference. The larger the value of RMS-DS, the greater the effect of inter-symbol interference.

3.8.4 Maximum Excess Delay

The maximum excess delay of a PDP is the time taken for multipath signal energy to fall to a value of X dB below the maximum of that particular PDP. It is given by

$$Max.Excess\_delay = \tau_x - \tau_0$$

Where τ_0 is the delay of the first multipath signal component and τ_x is the maximum value of delay at which the multipath signal component is within X dB from the maximum value.

3.9 Penetration Capacity and Ground

According to Electromagnetic theory, lower frequencies have better penetrating properties. The combination of larger spectrum and lower frequencies possessed by UWB makes it suitable for ground penetrating radar, foliage penetrating radar and short range radar to detect hidden objects behind walls. This penetration property is also of great importance for indoor geolocation systems [18]. Figure 3.1. Attenuation of EM signals through various materials as a function of frequency [19]. It can be seen in Figure 3.1 that the rate at which the attenuation of the radio signals occurs through various materials is very much a function of the kind of material. Certain materials like concrete block are sensitive to center frequencies, higher the center frequency higher is the attenuation. Use of high frequencies reduce the dimensions of receiver and 10 transmitter antennas but reduces the penetrating capability whereas use of lower frequencies enhances the penetration capability of EM waves through the wall but can reduce the Radar Cross Section (RCS) of the target when wavelength exceeds the size of the target. The FCC regulations for through wall imaging are less than 960 MHz or 1.99 to 10.6 GHz which satisfies both the requirement.

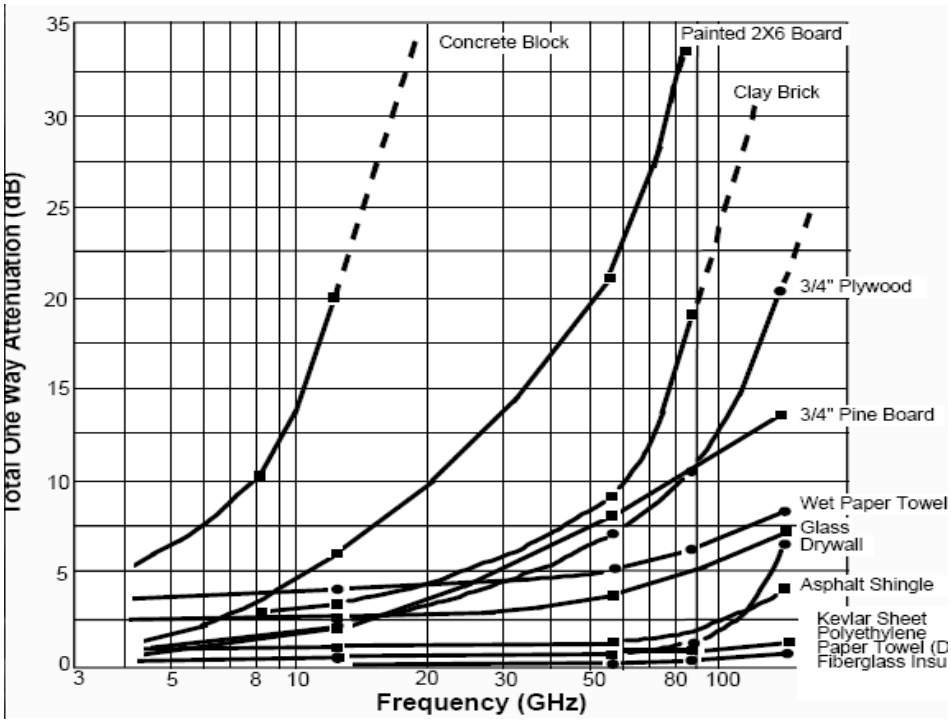

Figure 3-1 Attenuation of EM signals through various materials

as a function of frequency [19]

Chapter 4

EQUIPMENT CONFIGURATIONS AND MEASUREMENTS

The hardware used for our experiment is a PulsON 410. PulsON products have been developed by Time Domain Corporation based on Time modulated Ultra Wideband (TM-UWB) architecture. The usage of PulsON radar in the bistatic mode has been explained in this chapter and also some important terms associated with it. The waveform pulses are transmitted from a single Omni-directional antenna and the scattered waveforms are received by a collocated Omni-directional antenna. The two antenna ports on the P410 are used for transmit and receive antennas.

4.1 Using PlusON 410 – As Ranging and Communication Module (RCM)

The P410, shown in Figure 2.1, is a small, low power and affordable device which provides accurate, high rate range measurements and superior operational performance when compared to conventional RFID/RTLS devices. When used as a ranging radio, it is typically referred to as a P410 RCM.

Figure 4-1 P410 RCM with Broad spec antenna

A block diagram showing operation of a ranging and communication system is provided below

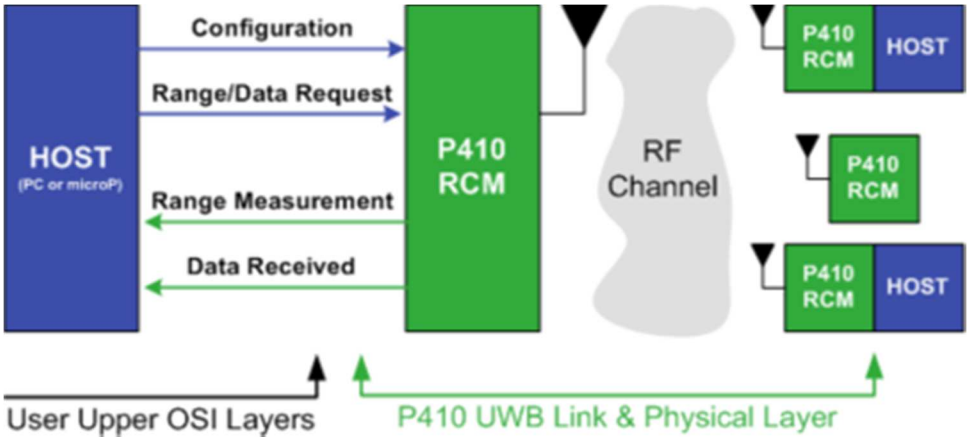

Figure 4-2 Block Diagram of P410 RCM

4.2 Key Features of the P410 RCM

- Excellent performance in high multipath and high clutter environments
- Coherent signal processing extends operating range
- Direct sequential pulse sampling allows measurement of received waveform (resultant waveform is available to the user for ranging optimization)
- Two-Way Time-of-Flight (TW-TOF) ranging technique provides highly precise range measurements with industry-leading update rate
- Coarse Range Estimation (CRE) technique estimates the range from a transmitting unit by using the received leading edge signal strength and periodically recalibrating the estimate based on infrequent TW-TOF range measurements
- UWB chipset enables low cost, small size, and low power operation
- UWB waveform and pseudo random encoding ensures noise-like transmissions with a very small RF footprint
- RF transmissions from 3.1 GHz to 5.3 GHz, with center at 4.3 GHz

4.3 Precision Range Measurement Technique

The P410 RCM uses two different techniques to measure the distance between devices. Two-Way Time-of-Flight (TW-TOF) offers high accuracy measurements as well as an estimate of the accuracy of each TW-TOF measurement. Such estimates can be used by a Kalman filter to more accurately report location. With TW-TOF, a P410 RCM sends a range request to another P410 RCM, which acknowledges the request with a range response. The initiating P410 RCM uses the response information to calculate the intervening distance with an accuracy of 2 cm. In Clear Line of Sight conditions, the P410 RCM also provides a Coarse Range Estimate (CRE) of the range. This measure is based

on the signal strength of the first arriving energy and is periodically recalibrated with TW-TOF measurements. While not as accurate as TW-TOF, CRE measurements can be used to increase system capacity by up to a factor of 7. Unlike ultrasonic or laser-based ranging techniques, UWB pulses can travel through walls and dense foliage. Also, unlike conventional narrow-band RF, these pulses do not suffer from errant multi-path reflections – the most direct path through the environment is measured [10]

4.4 Signal, Noise and SNR calculation

The SNR reported by RCM is based on an estimate of the signal and noise made by the P4xx and reported through the API. SNR is 20*Log10(Vpeak / Noise) where Vpeak is a measure of the largest signal near the leading edge of the scan and noise is an estimate of the noise prior to the leading edge. While both of these estimates are close, neither estimate is exact [10].

Consequently the measure of SNR is close, but not exact. First, SNR is actually computed from the scan measured during waveform generation after the receiver has acquired lock. Given that, the SNR is not the SNR the radio sees when it acquires the signal, but rather the SNR it sees during the waveform scan. However, these SNRs are believed to be close to each other.

Noise and signal are also imperfect estimates in the following senses. For example, the “proper” way of calculating noise might be based on computing the standard deviation of the 1300 readings which occur prior to the leading edge. For processor computation reasons a much simpler estimation process was used. This noise estimate has proven to be adequate and believe it is within 1-2dB of being accurate. In addition, Vpeak is the magnitude of the absolute value of the largest lobe. However, if the radio is not locked on the largest lobe then the receiver will be experiencing a smaller magnitude

signal. In those cases, the SNR reported can be a few dB higher than the SNR which the receiver is actually experiencing.

As a practical matter this SNR estimation process has proved to be a useful and repeatable, if slightly inaccurate, tool for describing radio performance. Users wishing more exact estimates of SNR can log scan waveforms and develop custom algorithms that yield more accurate results. As suggested earlier, SNR can be calculated directly from logged Scan Info. An example is offered below. It is more computationally intensive but still produces results within a dB of those produced by the P410 [10].

- Compute the standard deviation of the first 1337 entries in a Full Scan. This will produce statistics on the signal-free period that precedes the first arriving energy in a scan.
- Noise = 2*(Standard Deviation) ^2
- Unscaled Vpeak = Vpeak*(2^PII)/256 4) SNR = 10*log10 (Vpeak^2/Noise)

The above algorithm is used in the experiments to compute signal strength, SNR and noise floor.

The below few RCM-RET UI snap shots in Figure describes, roughly, the initial setup of the apparatus and software/hardware configurations. Figure 4-3 shows the settings of the CONFIGURATIONS tab, Figure 4-4 shows the settings of the SEND tab, Figure 4-5 shows the RECEIVE tab with data areas, Figure 4-6 shows the RANGE tab, which shows the TX-RX separation distance.

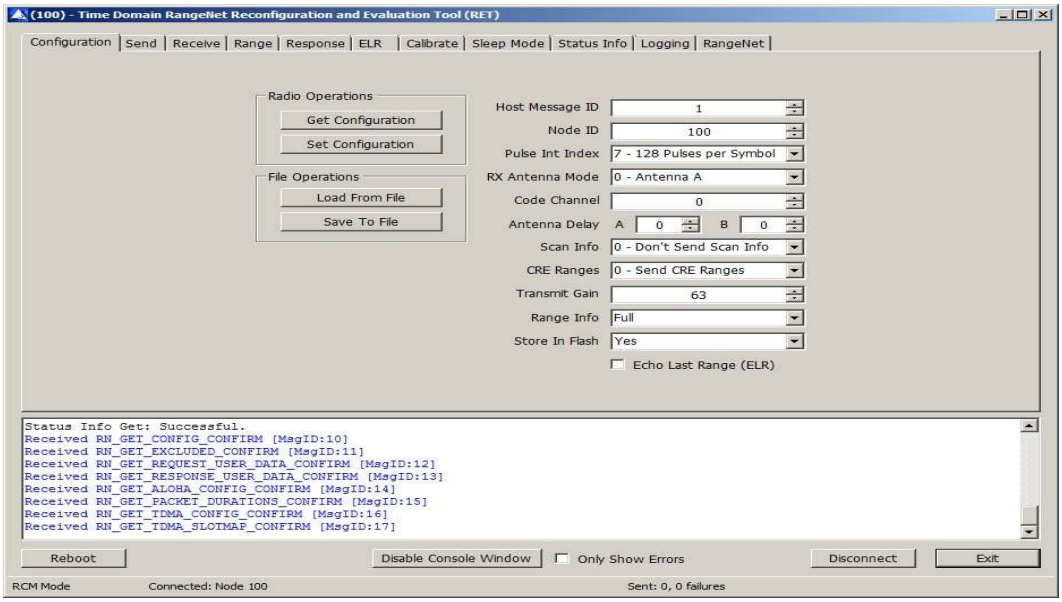

Figure 4-3 Configuration Tab featuring set up tab

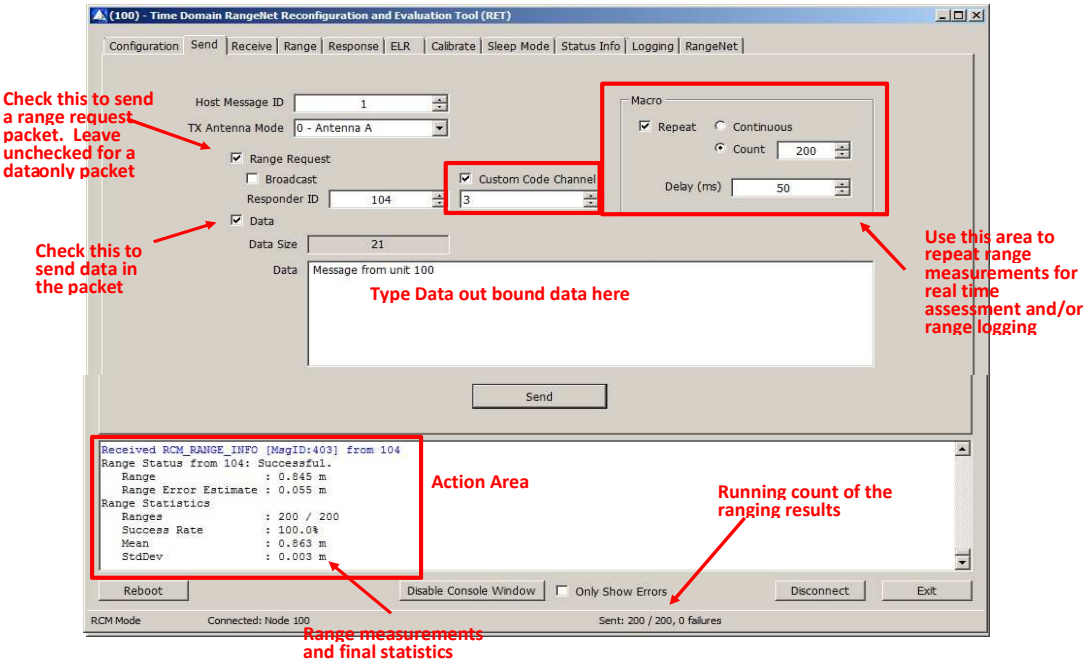

Figure 4-4 Send Tab showing results of a 200 measurement test

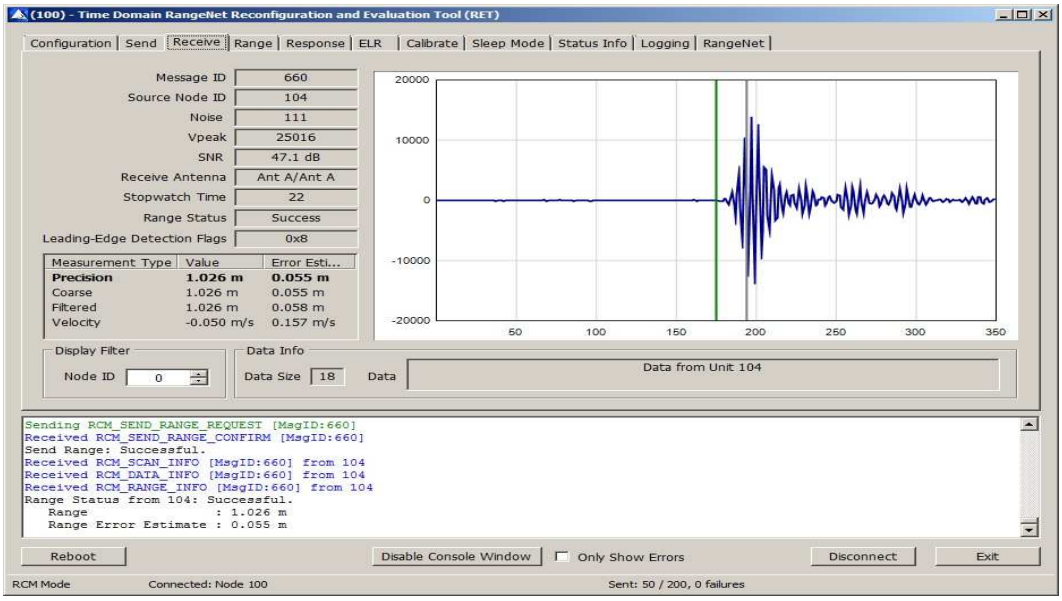

Figure 4-5 Receive Tab with data areas shown

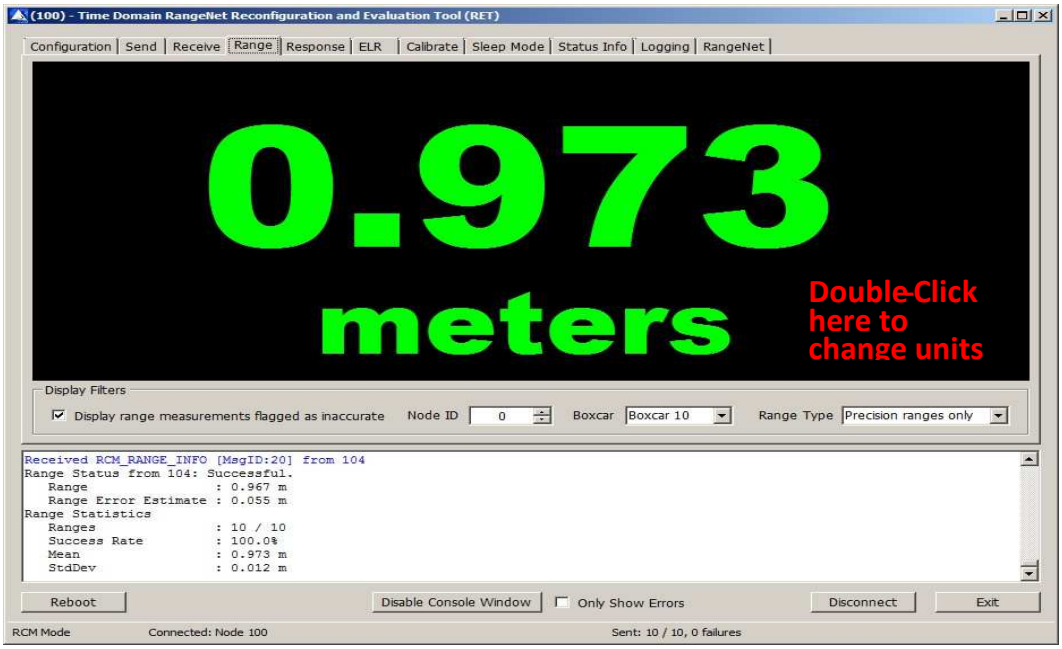

Figure 4-6 Range Tab displays TX-RX range measurement

Chapter 5

EXPERIMENTAL SCENARIOS, RESULTS AND ANALYSIS

5.1 Channel parameters for Brick wall corridor

Both the transmitter (TX) and receiver (RX) in both the experiments were placed at a height of 1 meter from the floor. The RX was moved by a human. During the conduct of the experiment there were two people involved, each one next to the TX and RX. The person sitting next to the TX was stationary and the other person was involved in moving the RX away from the TX in the corridor. This corridor includes many offices, labs, stairways and hallways each have either wooden doors or glass doors.

5.1.1 TX moving away from RX

5.1.1.1 Large scale parameters

The Figure (5-1) shows path loss data vs distance (10*log10*Distance in meters) in the brick wall corridor where the length of the corridor is 30 and 60 meters. The path loss exponent (n) was found to be 1.42. The Figure (5-2) shows the received signal strength, noise, and Signal to Noise Ratio (SNR) vs distance. Here the variation of the received UWB signal along the brick wall corridor is seen. Figure (5-3) shows the probability density function of generalized extreme value distribution (GEV) and normal distribution to the path loss data. Also in Figure (5-4) we show the difference in the cumulative distribution function between GEV and the normal distribution.

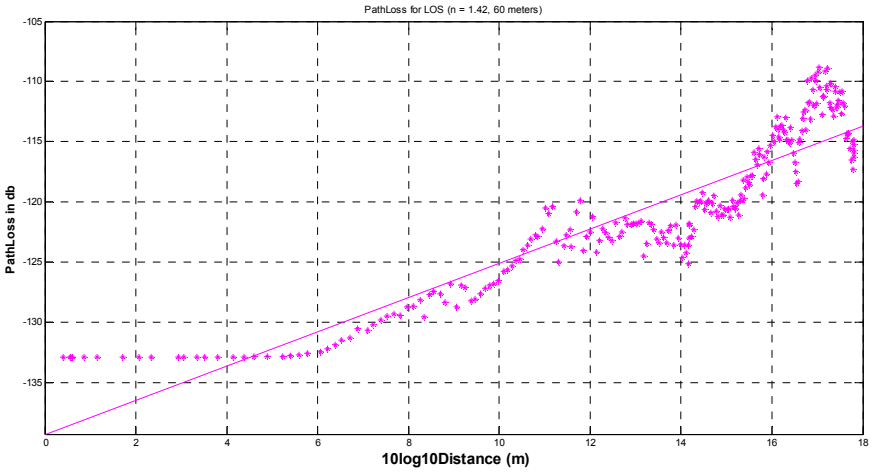

Figure 5-1 Path Loss vs Distance

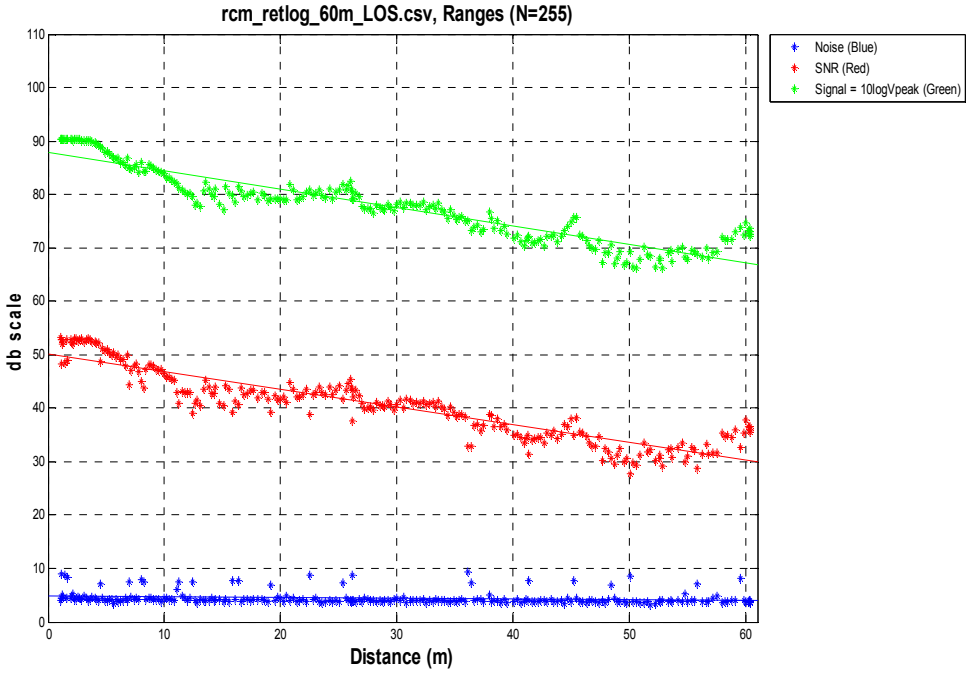

Figure 5-2 SNR, Signal Strength & Noise (dB) vs Distance (m)

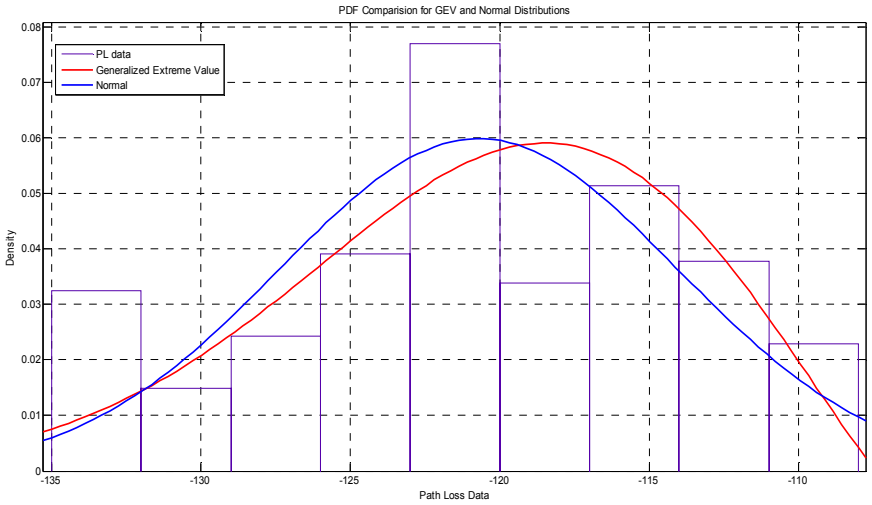

Figure 5-3 PDF Comparison b/w GEV and Normal Distributions

Table 5-1 Comparison between distributions (for 5.1.1)

	GEV	Normal
Log likelihood	-810.591	-818.677
Mean	-120.709	-120.712
variance	44.1411	44.4842

Table 5-2 distribution parameter estimates of GEV distribution (for 5.1.1)

Parameter	Estimate	Std. Err.
k	-0.47287	0.051632
sigma	7.13521	0.396863
mu	-122.434	0.505155

Table 5-3 estimated covariance of
GEV distribution (for 5.1.1)

	k	sigma	mu
k	0.0026659	-0.0141117	-0.0111295
sigma	-0.0141117	0.1575	-0.0287858
mu	-0.0111295	-0.0287858	0.255181

Table 5-4 distribution parameter estimates of
Normal distribution (for 5.1.1)

Parameter	Estimate	Std. Err.
mu	-120.712	0.42438
sigma	6.66965	0.300997

Table 5-5 estimated covariance of
Normal distribution (for 5.1.1)

	mu	sigma
mu	0.180098	1.31E-15
sigma	1.31E-15	0.0905992

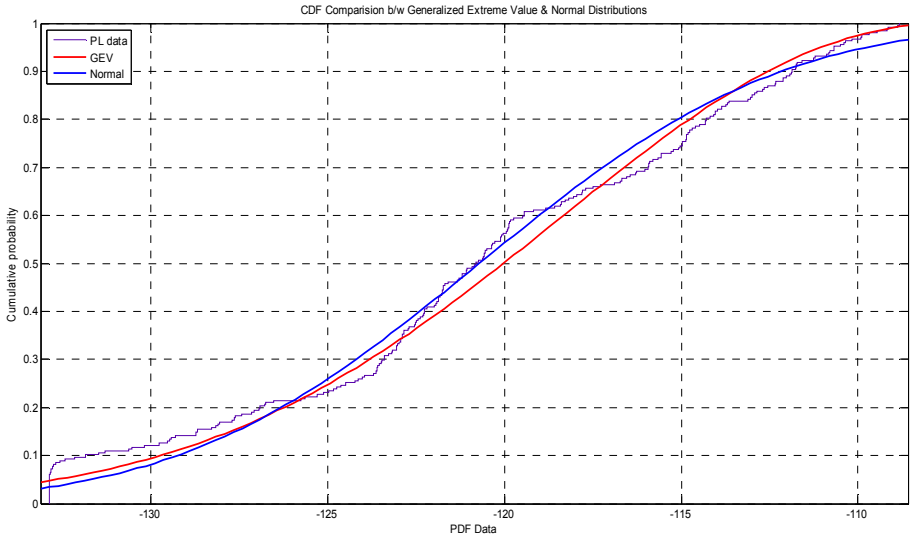

Figure 5-4 Cumulative Density Functions for 5.1.1

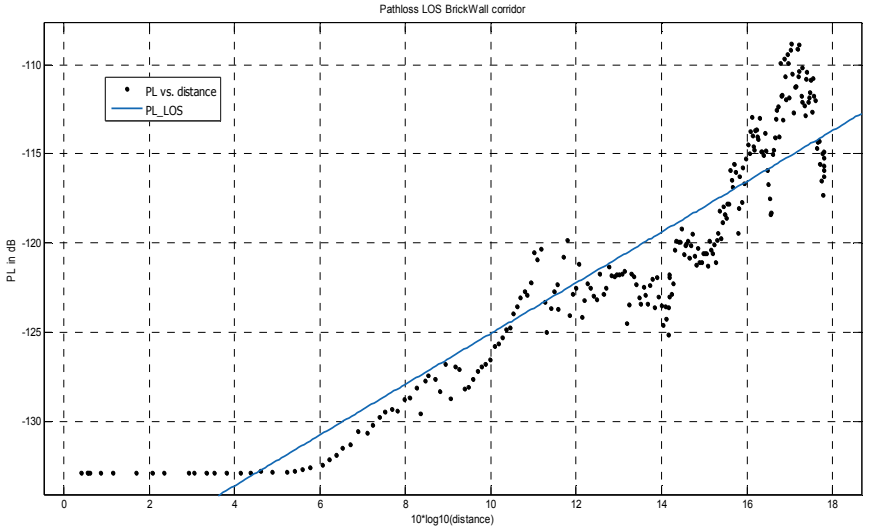

Figure 5-5 Path loss exponent for 5.1.1

General model: Calculated from equation (3.5)

F (distance) = -1.328806065617482e+02 + n*distance + y*s

Coefficients (with 95% confidence bounds):

n = 1.42 (1.345, 1.495)

s = -2.468 (-3.839e+06, 3.839e+06)

y = 2.587 (-4.023e+06, 4.023e+06)

Goodness of fit:

SSE: 1597

R-square: 0.8541

Adjusted R-square: 0.8529

RMSE: 2.558

5.1.1.2 Small scale parameters

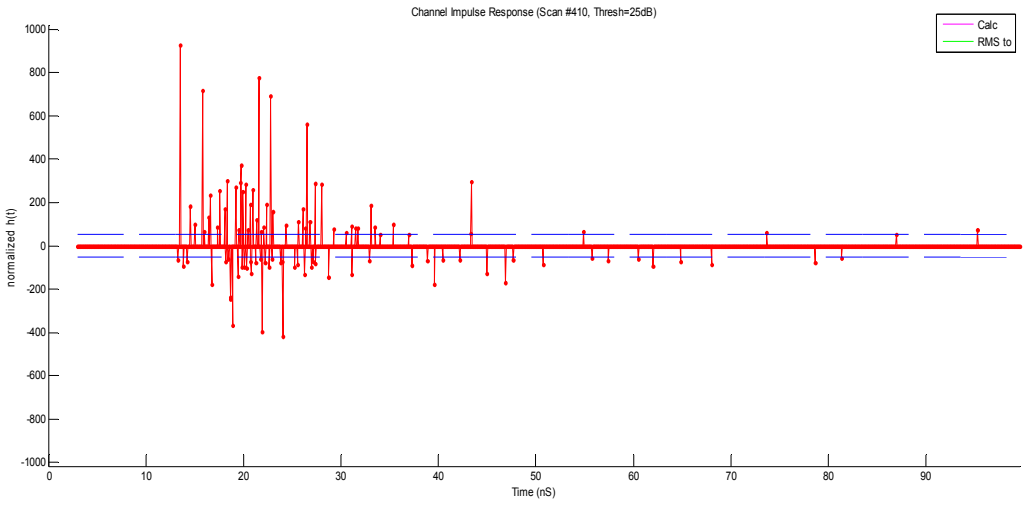

Figure 5-6 CIR for 5.1.1

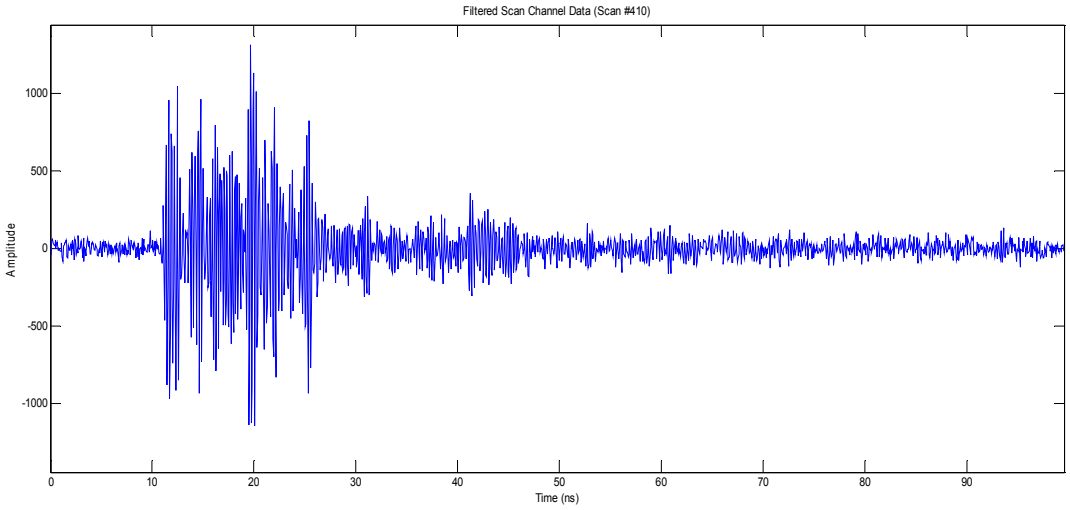

Figure 5-7 Filtered Data for 5.1.1

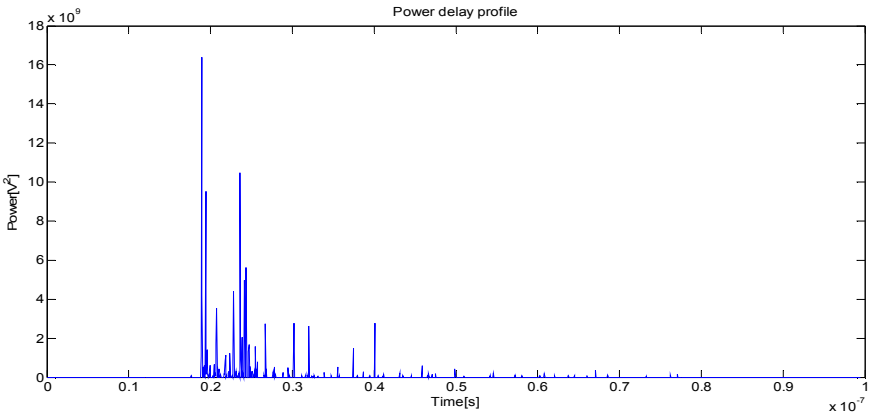

Figure 5-8 PDP for 5.1.1

Mean_excess_delay = 8.1805 ns

Average RMS Delay spread = 11.4657 ns

Maximum RMS Delay spread = 22.3598

Minimum RMS Delay spread = 0.5692

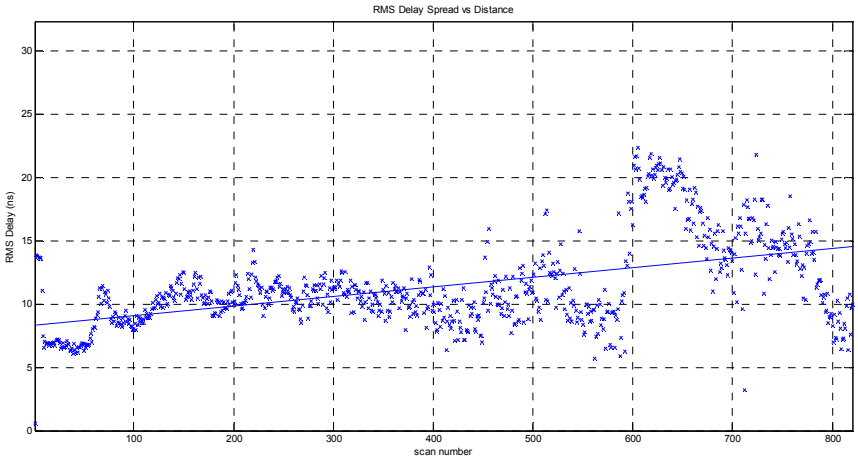

Figure 5-9 RMSDS for 5.1.1

5.1.2 TX moving towards RX

5.1.2.1 Small scale parameters

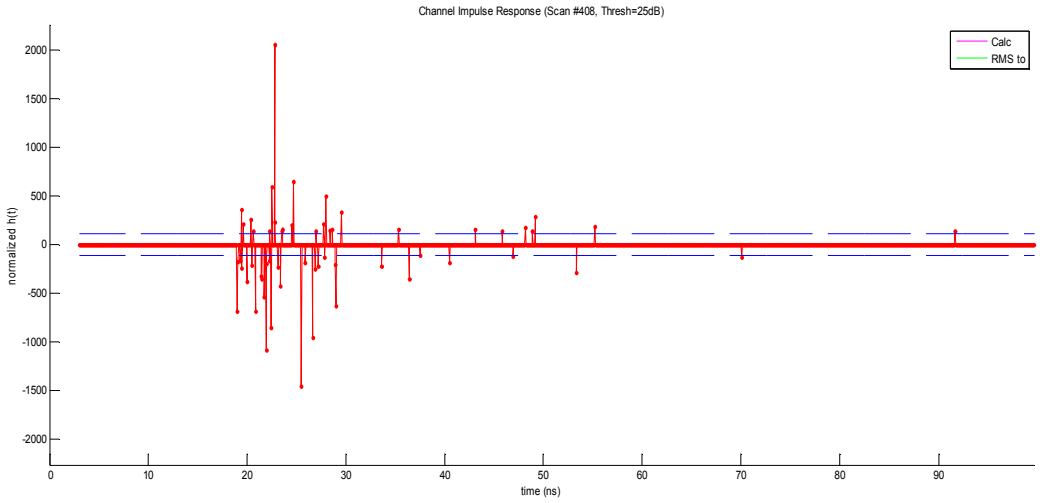

Figure 5-10 CIR for 5.1.2

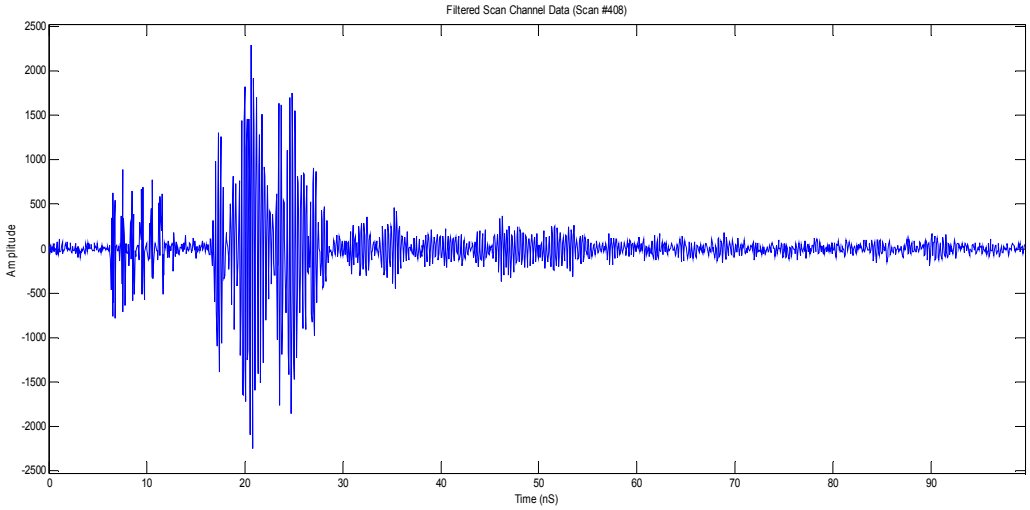

Figure 5-11 Filtered Data for 5.1.2

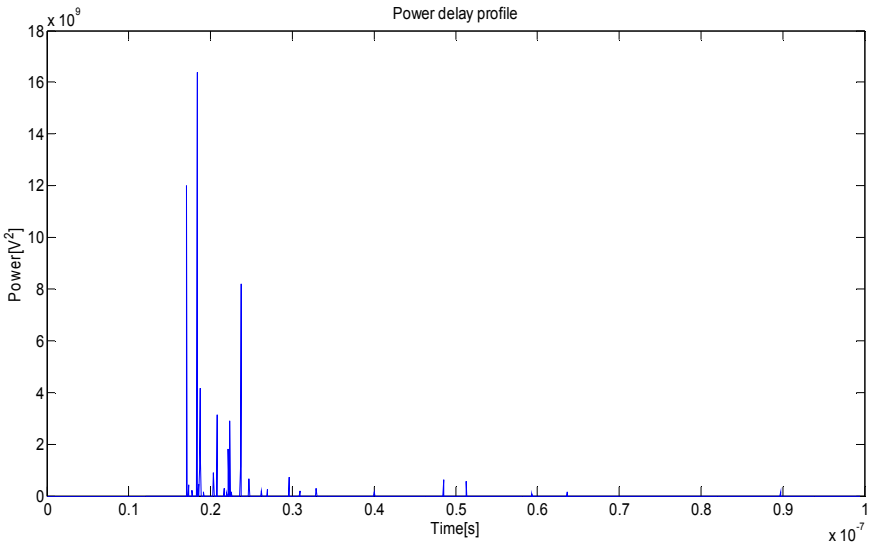

Figure 5-12 PDP for 5.1.2

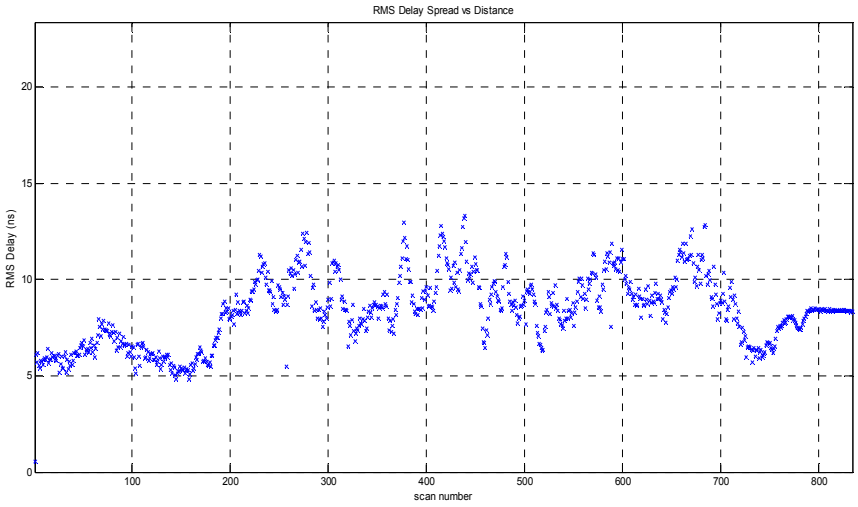

Figure 5-13 RMSDS for 5.1.2

Mean_excess_delay = 5.2655 ns

Average RMS Delay spread = 8.3689 ns

Maximum RMS Delay spread = 13.3266 ns

Minimum RMS Delay spread = 0.5692 ns

5.2 Channel parameters for Gypsum wall corridor

5.2.1 TX moving away from RX

5.2.1.1 Large scale parameters

The Figure (5.14) shows path loss data (dB) vs distance (10*log10*Distance in meters) in a Gypsum wall corridor and the length of the corridor is 30 meters. The path loss exponent (n) was found to be 1.1. The Figure (5.15) shows the received signal strength, Noise, and Signal to Noise Ratio (SNR) vs Distance. Here the variation of the received UWB signal along the brick wall corridor is seen. Figure (5.16) shows the probability density function of generalized extreme value distribution (GEV) and the normal distribution to the

path loss data. Also in Figure (5.17) we show difference in cumulative distribution function between GEV and the normal distribution.

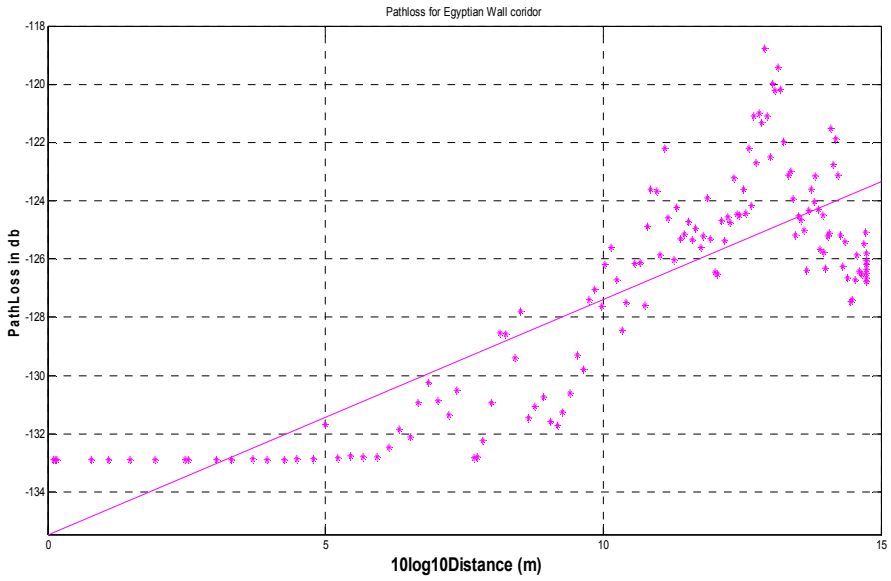

Figure 5-14 Path loss data for 5.2.1

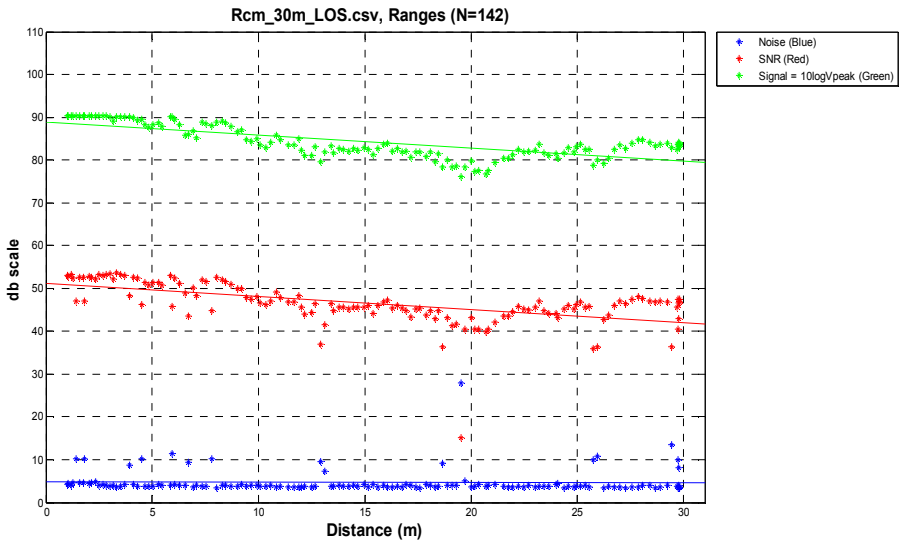

Figure 5-15 SNR, Signal Strength & Noise (dB) vs Distance (m)

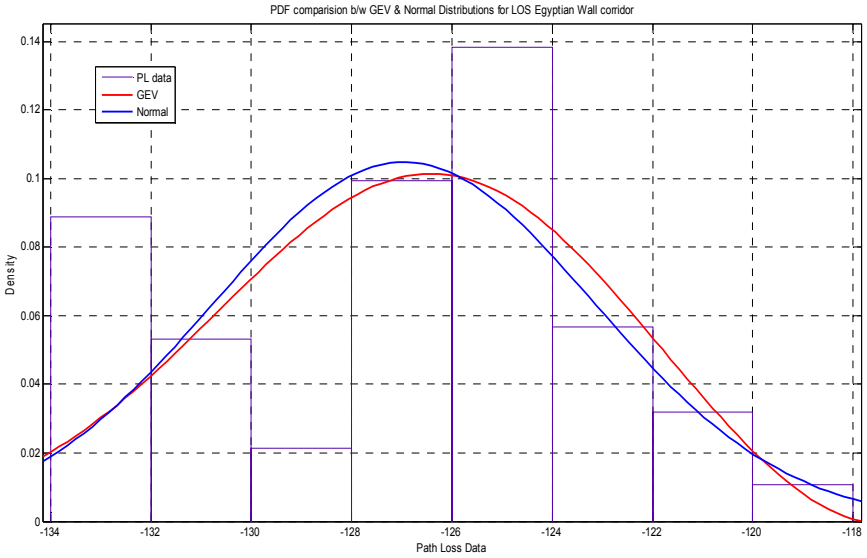

Figure 5-16 PDF Comparison b/w GEV and Normal Distributions

Table 5-6 Comparison between distributions (for 5.2.1)

	GEV	Normal
Log likelihood	-385.438	-388.082
Mean	-126.969	-126.958
variance	14.1972	14.4967

Table 5-7 distribution parameter estimates of GEV distribution (for 5.2.1)

Parameter	Estimate	Std. Err.
k	-0.378374	0.0504674
sigma	3.94046	0.265044
mu	-128.128	0.362021

Table 5-8 estimated covariance of GEV distribution (for 5.2.1)

	k	sigma	mu
k	0.00254696	-0.00876839	-0.00688964
sigma	-0.00876839	0.0702481	-0.0104724
mu	-0.00688964	-0.0104724	0.131059

Table 5-9 distribution parameter estimates of Normal distribution (for 5.2.1)

Parameter	Estimate	Std. Err.
mu	-126.958	0.320645
sigma	3.80745	0.227946

Table 5-10 estimated covariance of
Normal distribution (for 5.2.1)

	mu	sigma
mu	0.102813	1.33758e-16
sigma	1.33758e-16	0.0519593

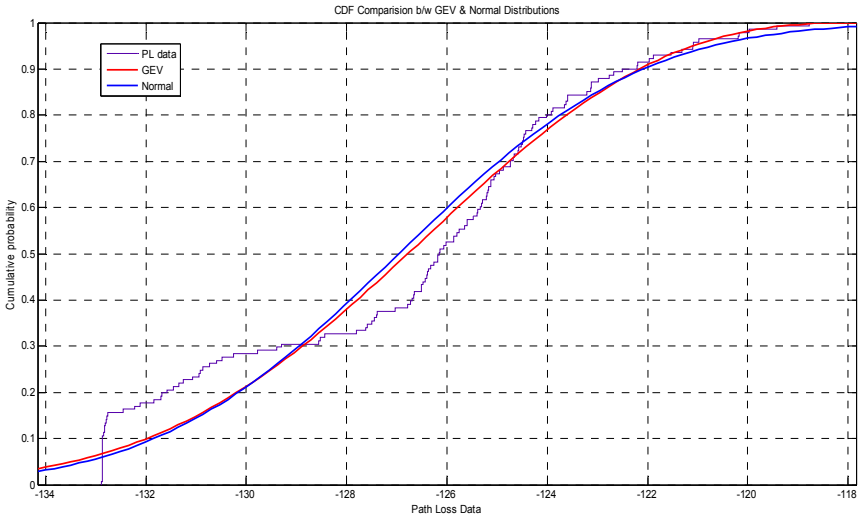

Figure 5-17 Cumulative Density Functions for 5.2.1

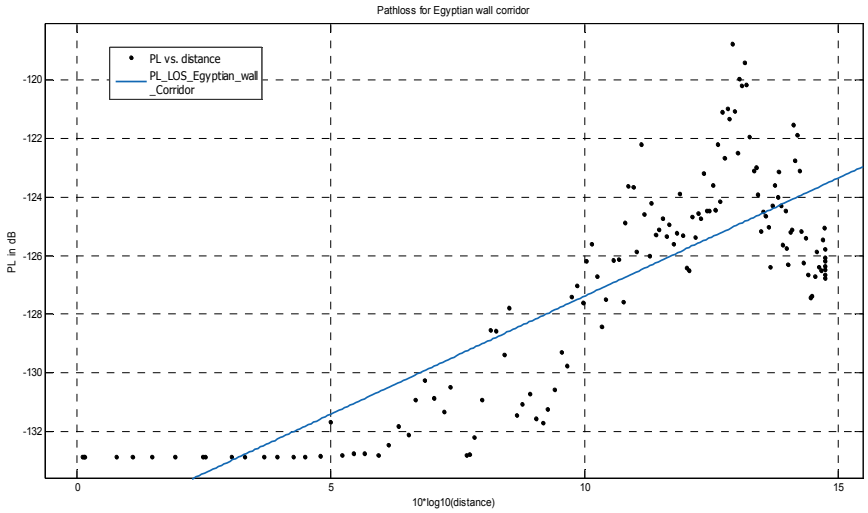

Figure 5-18 Path loss exponent for 5.2.1

General model: Calculated from equation (3.5)

F (distance) = -1.328806065617482e+02 + n*distance + y*s

Coefficients (with 95% confidence bounds):

n = 1.100 (0.7077, 0.9068)

s = 1.218 (-1.35e+15, 1.35e+15)

y = -2.113 (-2.343e+15, 2.343e+15)

Goodness of fit:

SSE: 657.9

R-square: 0.6758

Adjusted R-square: 0.6711

RMSE: 2.183

5.2.1.2 Small scale parameters

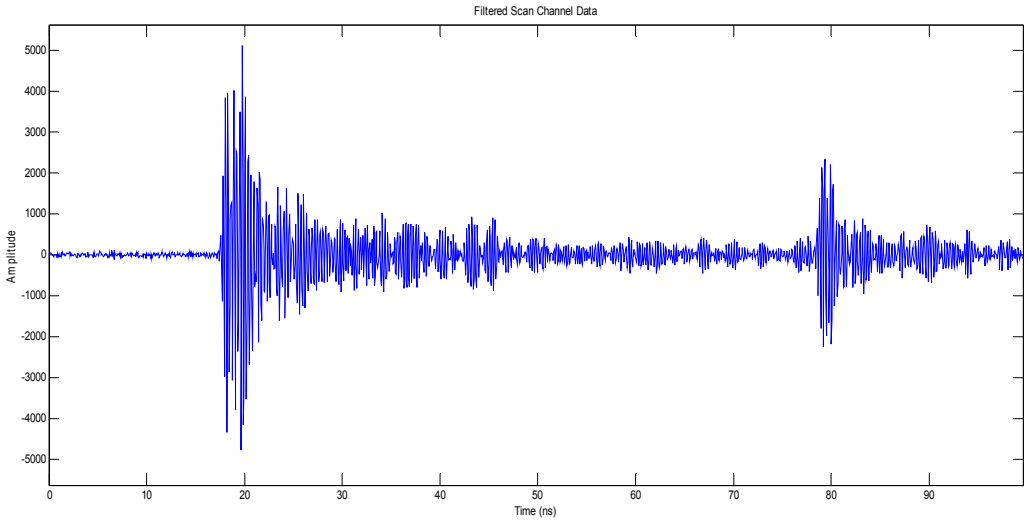

Figure 5-19 PDP 5.2.1

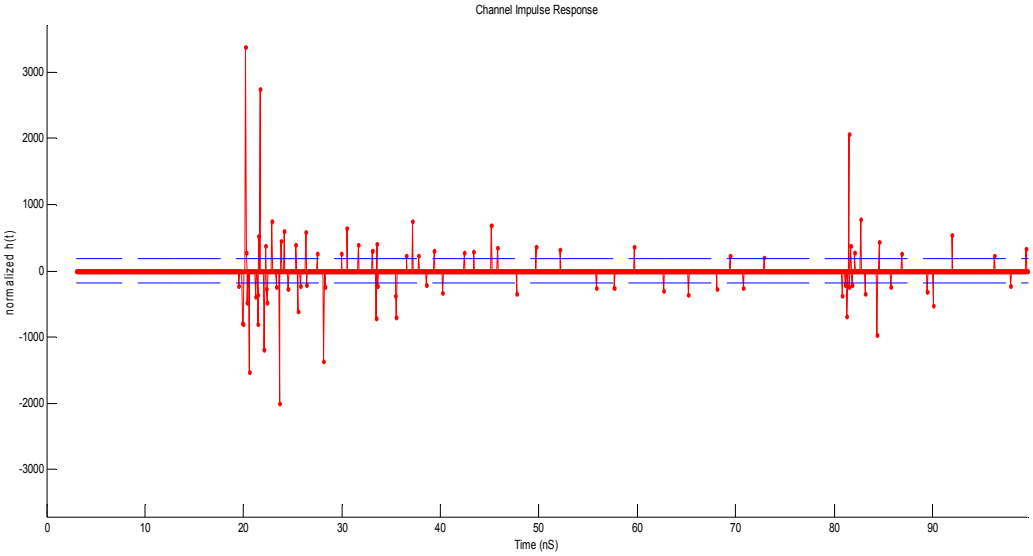

Figure 5-20 PDP 5.2.1

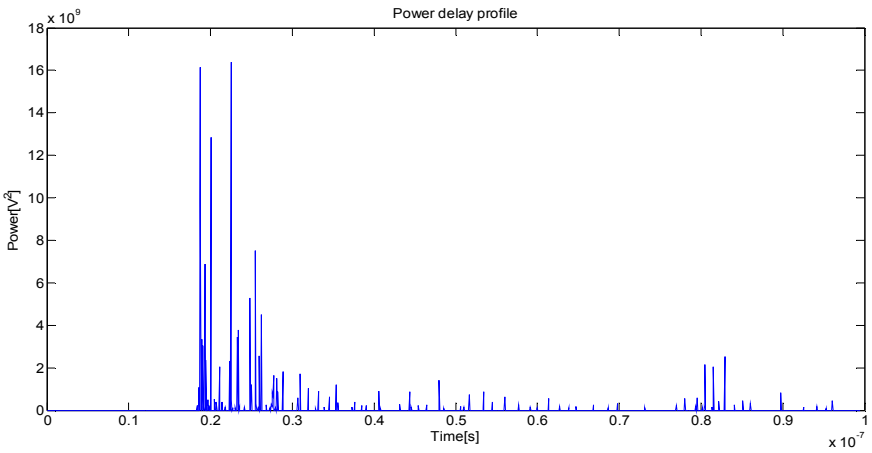

Figure 5-21 PDP 5.2.1

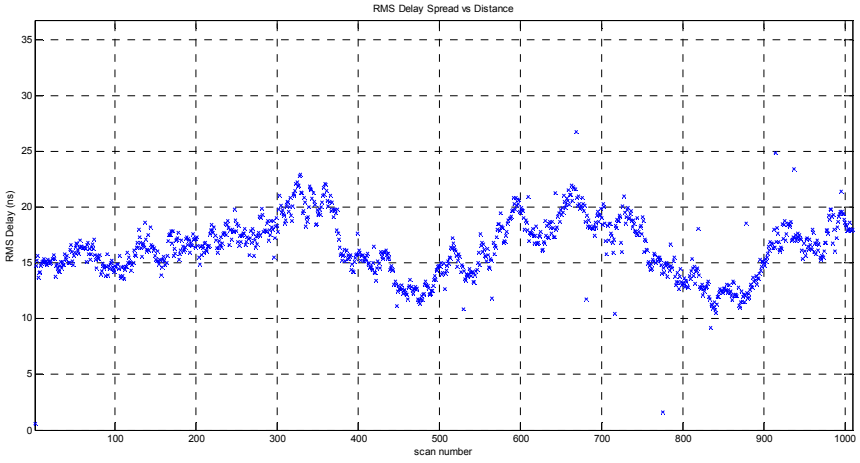

Figure 5-22 RMSDS 5.2.1

Mean_Excess_Delay = 9.4631 ns

Average RMS Delay Spread = 16.3544 ns

Maximum RMS Delay Spread = 26.7763 ns

Minimum RMS Delay Spread = 0.5692 ns

5.2.2 TX moving towards RX

5.2.2.1 Small scale parameters

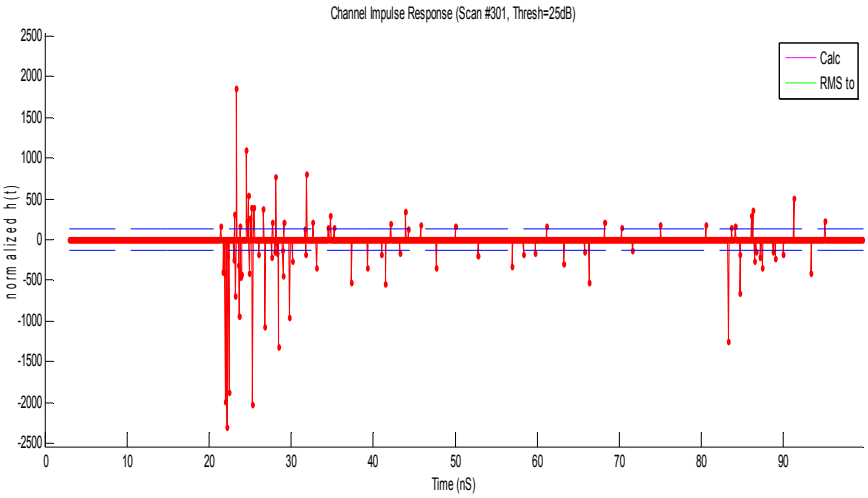

Figure 5-23 CIR 5.2.2

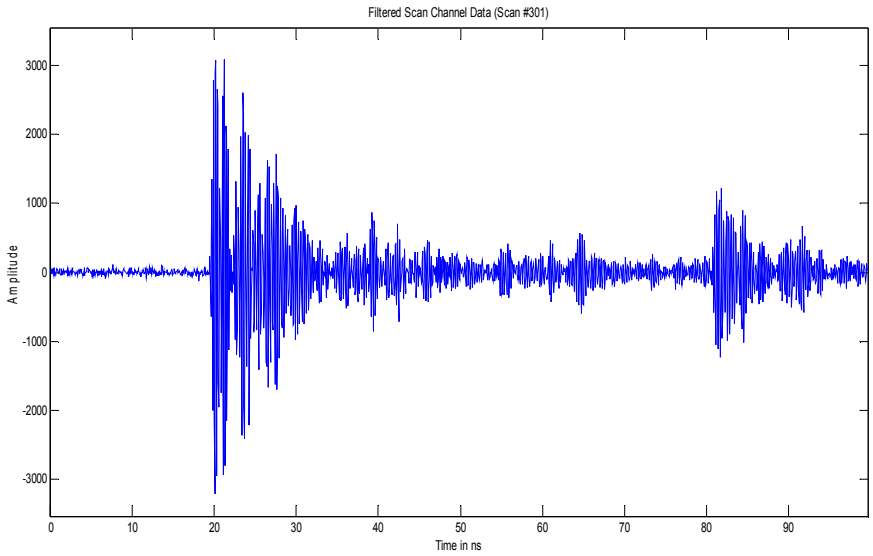

Figure 5-24 Filtered data channel 5.2.2

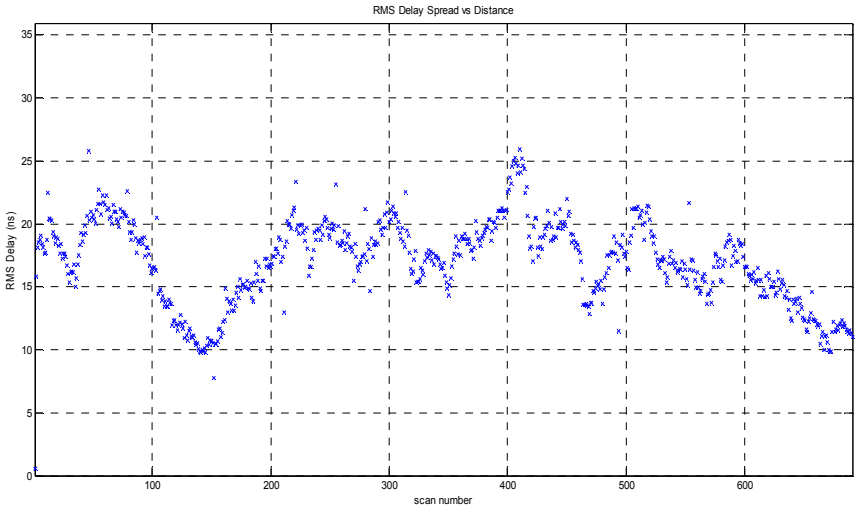

Figure 5-25 RMSDS 5.2.2

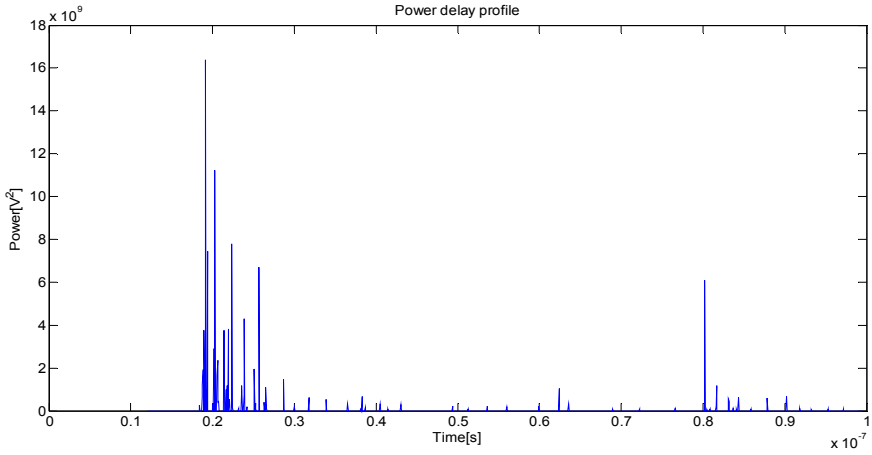

Figure 5-26 PDP 5.2.2

Mean_Excess_Delay = 10.1810 ns

Average RMS Delay Spread = 17.0580 ns

Maximum RMS Delay Spread = 25.9434 ns

Minimum RMS Delay Spread = 0.5692 ns

5.3 Channel parameters for through the walls Gypsum wall- Classroom environment

5.3.1 Through the wall (1 wall)

- The experiment was conducted in a classroom environment. The classrooms, NH 202 & NH 203 are adjacent to each other in 2nd floor of Nedderman Hall. The classrooms are separated by a Gypsum wall of thickness (30cm).
- TX & RX was in NH 202 & 203 respectively, both the antennae was at 2m height from the ground. TX was stationary at a distance of 4meters from the wall in NH 202.
- RX was moved from 5meters to 15 meters away from the TX in NH 203 classroom.
- The channel parameters are modeled below.

5.3.1.1 Large scale parameters

The Figure (5.25) shows path loss data vs distance (10*log10*Distance in meters) in a Gypsum wall corridor and the length of the corridor is 30 meters. The path loss exponent (n) was found to be 2.1. The Figure (5.26) shows the received signal strength, noise, and Signal to Noise Ratio (SNR) vs distance. Here the variation of the received UWB signal along the brick wall corridor is seen. Figure (5.27) shows the probability density function of generalized extreme value distribution (GEV) and normal distribution to the path loss data. Also in Figure (5.28) we show difference in cumulative distribution function between GEV and Normal distribution.

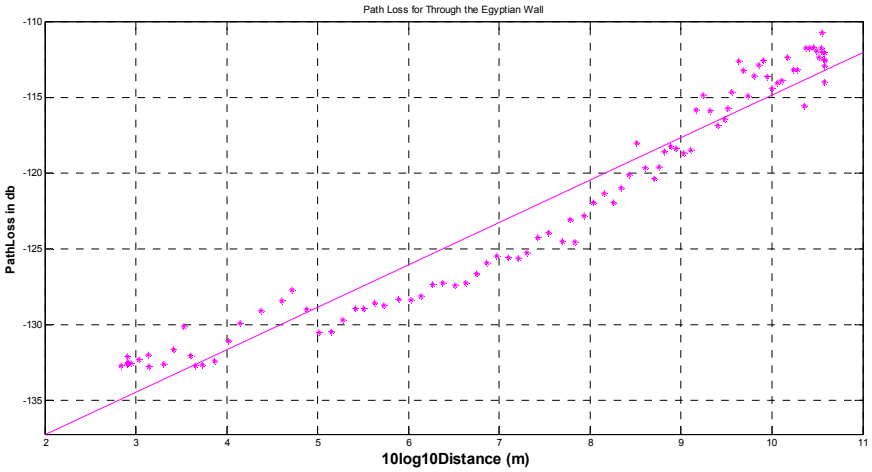

Figure 5-27 Path loss data for 5.3.1

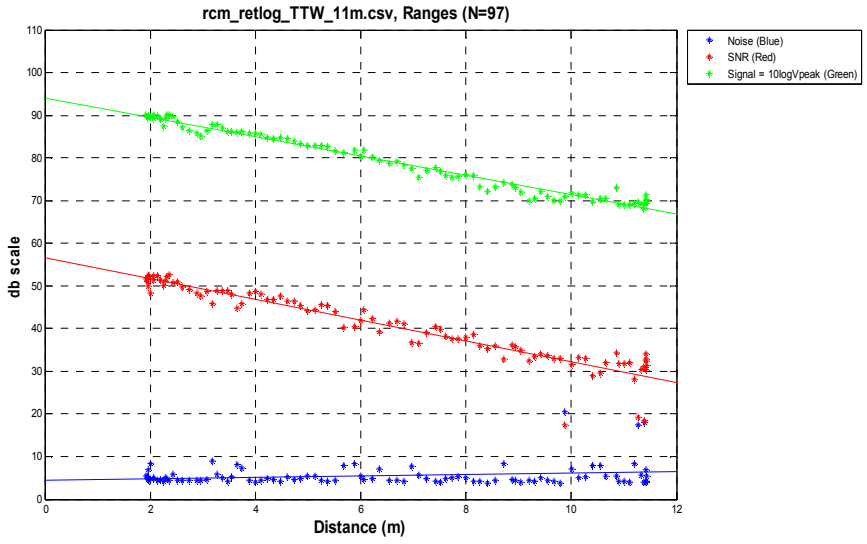

Figure 5-28 SNR, Signal Strength & Noise (dB) vs Distance (m)

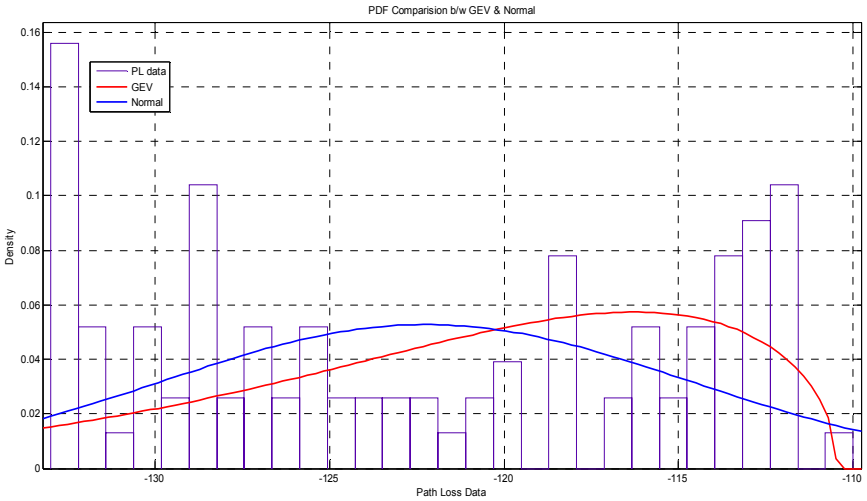

Figure 5-29 PDF Comparison b/w GEV and Normal Distributions

Table 5-11 Comparison between distributions (for 5.3.1)

	GEV	Normal
Log likelihood	-327.988	-333.352
Mean	-122.16	-122.235
variance	66.8378	57.1498

Table 5-12 distribution parameter estimates of

EV distribution (for 5.3.1)

Parameter	Estimate	Std. Err.
k	-0.6887	0.0896141
sigma	8.87688	0.914388
mu	-123.364	0 .979441

Table 5-13 estimated covariance of
GEV distribution (for 5.3.1)

	k	sigma	mu
k	0.00803068	-0.0574301	-0.0342089
sigma	-0.0574301	0.836105	-0.307837
mu	- 0.0342089	-0.307837	0.959304

Table 5-14 distribution parameter estimates of
Normal distribution (for 5.3.1)

Parameter	Estimate	Std. Err.
mu	-122.235	0.767576
sigma	7.55975	0.547004

Table 5-15 estimated covariance of
Normal distribution (for 5.3.1)

	mu	sigma
mu	0. 589173	3.54523e-15
sigma	3.54523e-15	0.299214

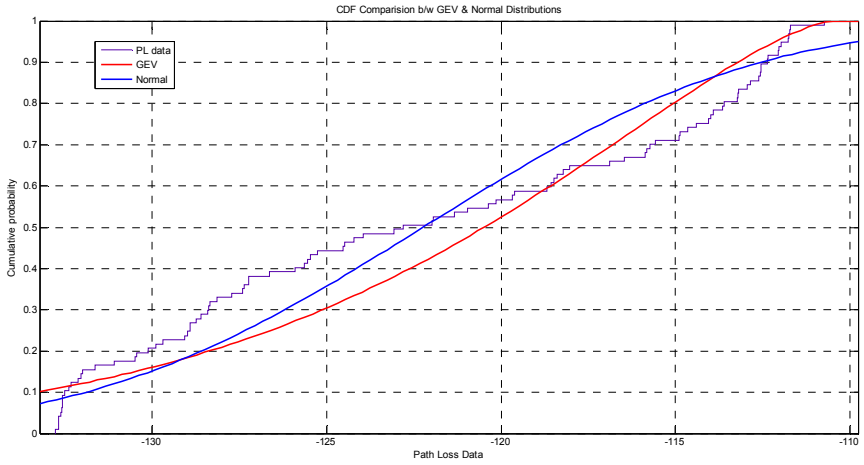

Figure 5-30 Cumulative Density Functions for 5.3.1

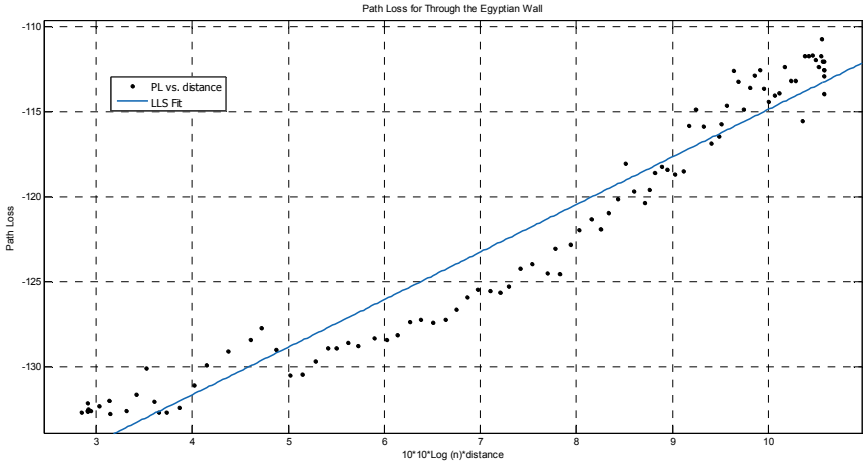

Figure 5-31 Path loss exponent for 5.3.1

General model: Calculated from (3.5)

F (distance) = -1.244175991221610e+02 + n*distance + Y*s

Coefficients (with 95% confidence bounds):

Y = -4.29 (-3.763e+06, 3.763e+06)

n = 2.195 (2.644, 2.945)

s = 4.288 (-3.761e+06, 3.761e+06)

Goodness of fit:

SSE: 314.1

R-square: 0.9428

Adjusted R-square: 0.9415

RMSE: 1.828

5.3.1.2 Small Scale parameters

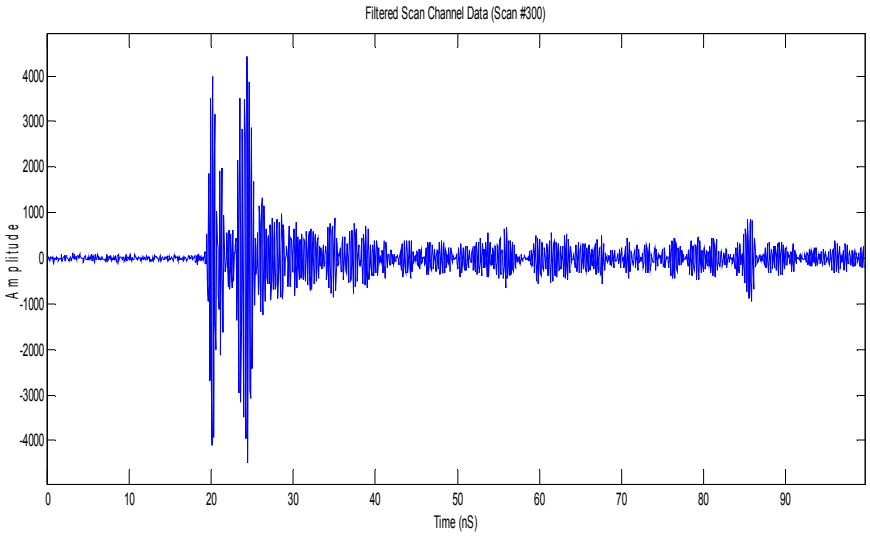

Figure 5-32 Filtered data for 5.3.1

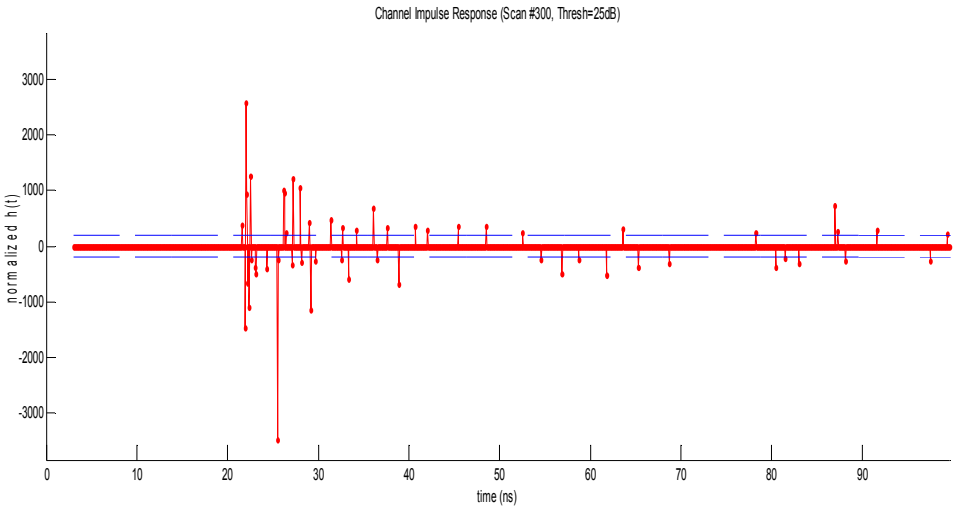

Figure 5-33 CIR for 5.3.1

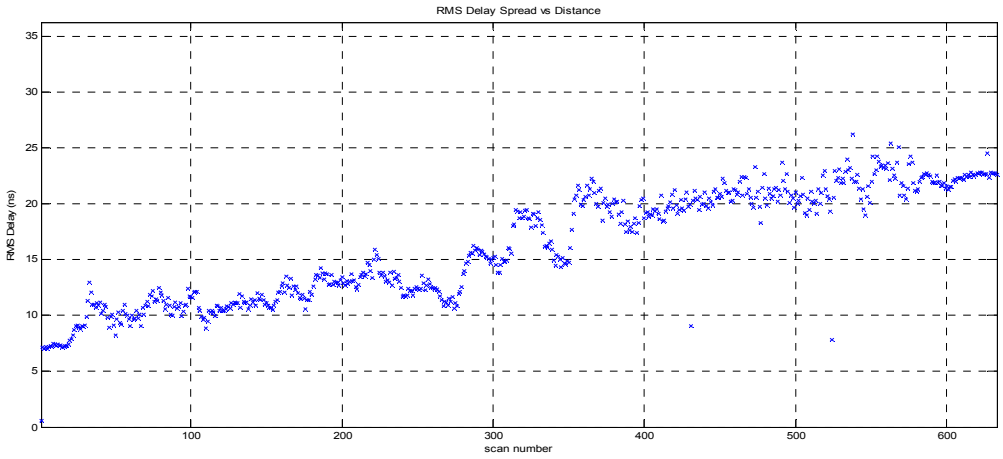

Figure 5-34 RMSDS for 5.3.1

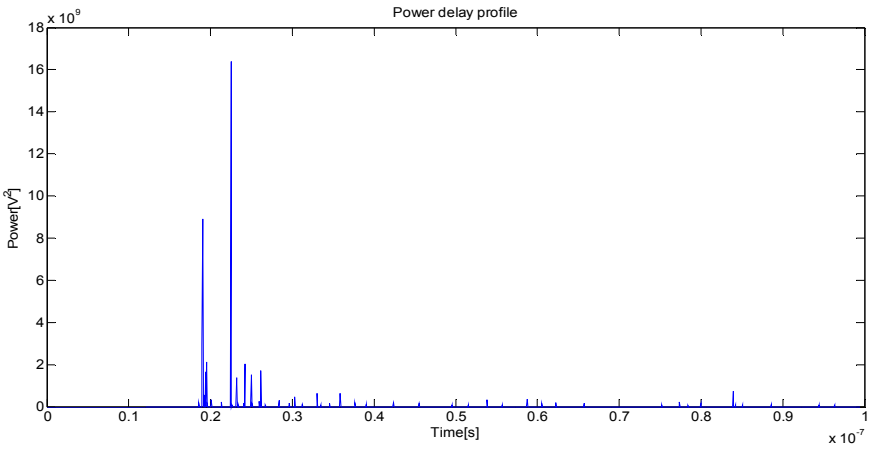

Figure 5-35 PDP for 5.3.1

Average RMS delay spread = 16.1977 ns

Maximum RMS delay spread = 26.2914 ns

Minimum RMS delay spread = 0.5692 ns

Mean_Excess_delay = 12.2504 ns

5.3.2 Through the walls (2 wall)

- This experiment was conducted in a classroom environment. The classrooms, NH 202 & NH 203 are adjacent to each other in 2nd floor of Nedderman Hall. The classrooms are separated by 2 walls Gypsum walls each of thickness of thickness (30cm).
- TX & RX was in NH 202 & hallway respectively, both the antennae was at 2m height from the ground. TX was stationary at a distance of 4meters from the wall in NH 202.
- RX was moved from 15meters to 30 meters away from the TX.
- The channel parameters are modeled below.

5.3.2.1 Large scale parameters

The Figure (5.34) shows path loss data (dB) vs distance (10*log10*Distance in meters) in a Gypsum wall corridor and the length of the corridor is 30 meters. The path loss exponent (n) was found to be 2.1. The Figure (5.35) shows the received signal strength, noise, and Signal to Noise Ratio (SNR) vs distance. Here the variation of the received UWB signal along the brick wall corridor is seen. Figure (5.36) shows the probability density function of generalized extreme value distribution (GEV) and normal distribution to the path loss data. Also in Figure (5.37) we show difference in cumulative distribution function between GEV and the normal distribution.

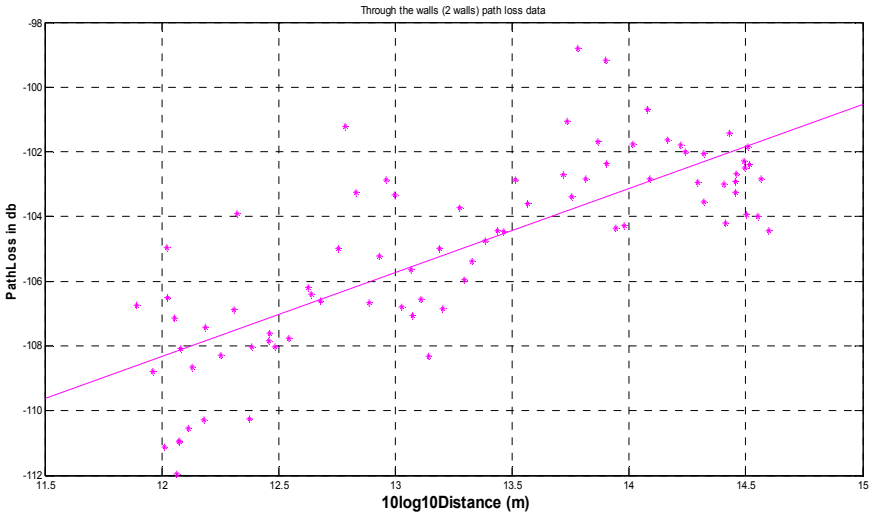

Figure 5-36 Path loss data for 5.3.2

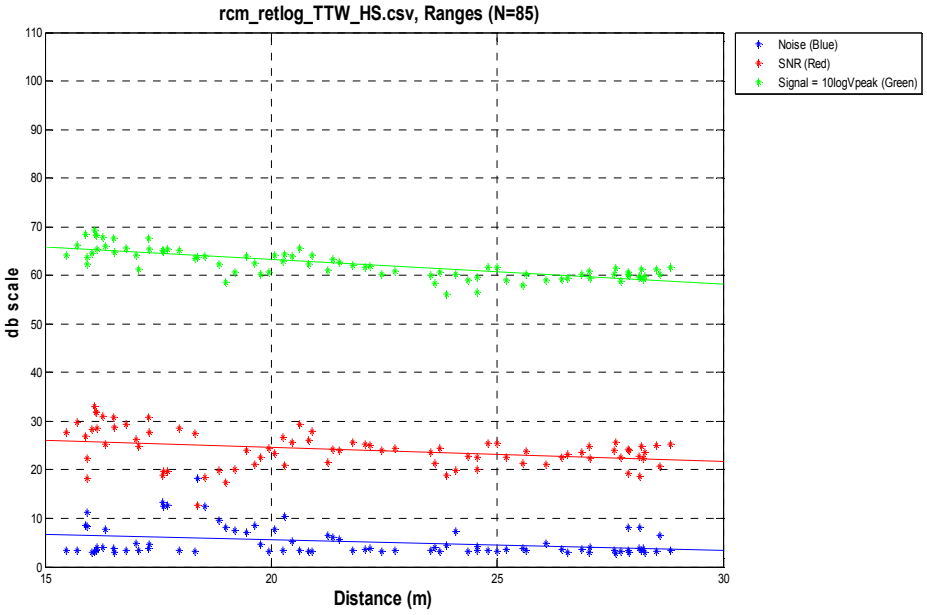

Figure 5-37 SNR, Signal Strength & Noise (dB) vs Distance (m)

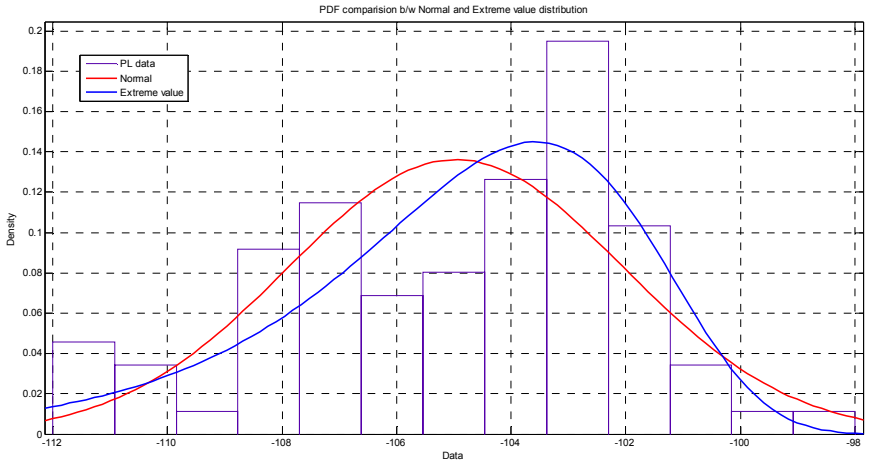

Figure 5-38 PDF Comparison b/w EV and Normal Distributions

Table 5-16 Comparison between distributions (for 5.3.2)

	EV	Normal
Log likelihood	-200.936	-201.529
Mean	-105.037	-104.966
variance	10.598	8.58899

Table 5-17 distribution parameter estimates of

EV distribution (for 5.3.2)

Parameter	Estimate	Std. Err.
mu	-103.572	0.297997
sigma	2.53827	0.213479

Table 5-18 distribution parameter estimates of

Normal distribution (for 5.3.2)

	mu	sigma
mu	-104.966	0.325633
sigma	2.9307	0.232419

Table 5-19 estimated covariance of

Normal distribution (for 5.3.2)

	mu	sigma
mu	0.106037	1.04912e-15
sigma	1.04912e-15	0.0540188

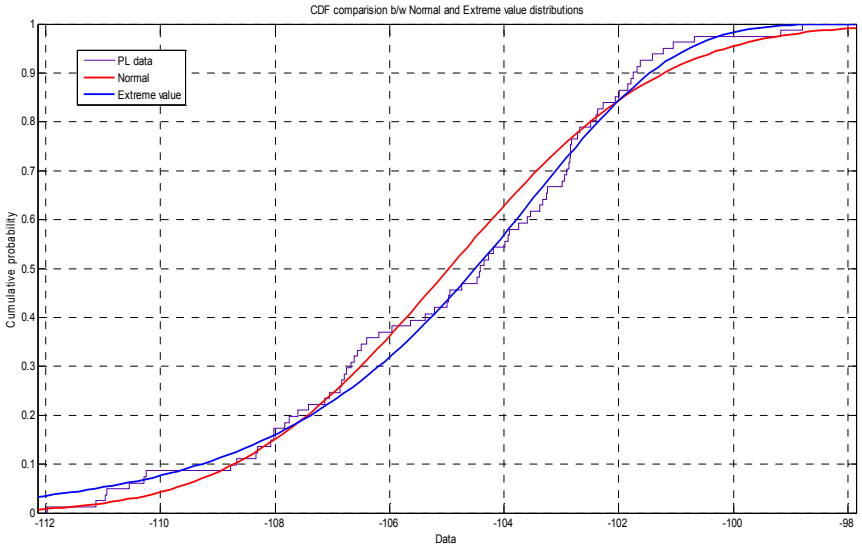

Figure 5-39 Cumulative Density Functions for 5.3.2

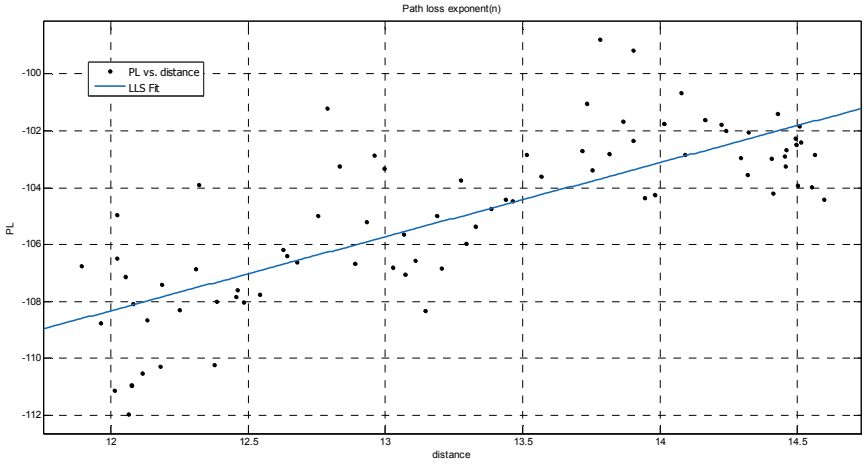

Figure 5-40 Path loss exponent for 5.3.2

General model: Calculated from (3.5)

F (distance) = -1.244175991221610e+02 + n*distance + Y*s

Coefficients (with 95% confidence bounds):

Y = -4.037 (-2.528e+14, 2.528e+14)

n = 2.603 (2.129, 3.076)

s = 3.751 (-2.349e+14, 2.349e+14)

Goodness of fit:

SSE: 267

R-square: 0.6114

Adjusted R-square: 0.6015

RMSE: 1.85

5.3.2.2 Small scale parameters

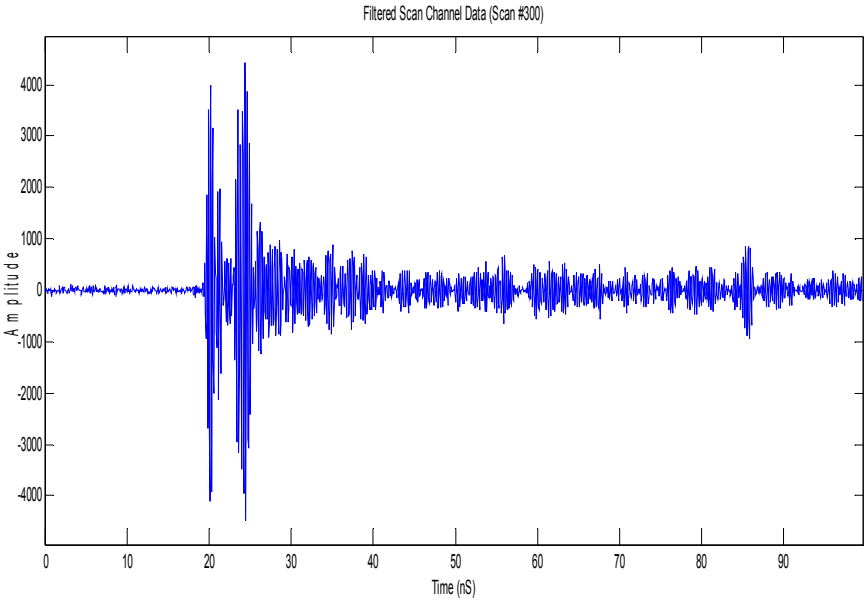

Figure 5-41 Filtered Data for 5.3.2

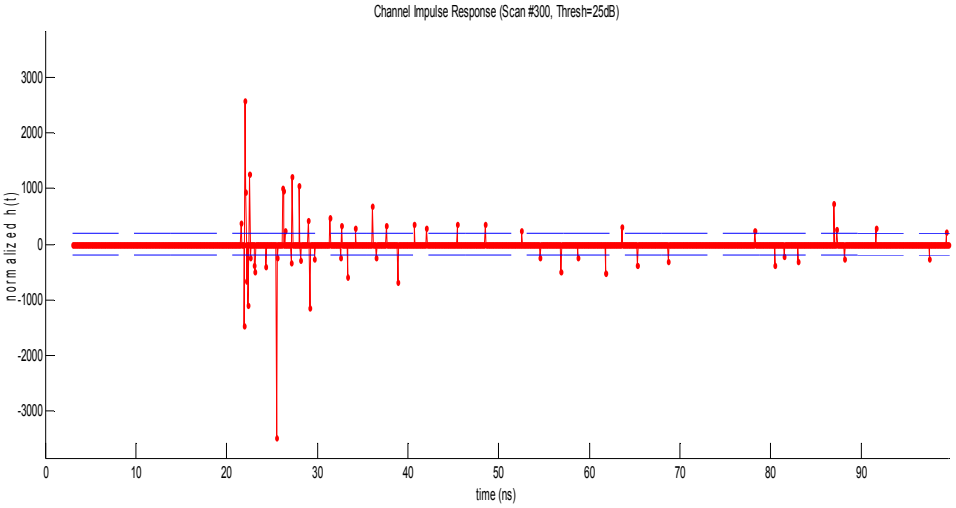

Figure 5-42 CIR for 5.3.2

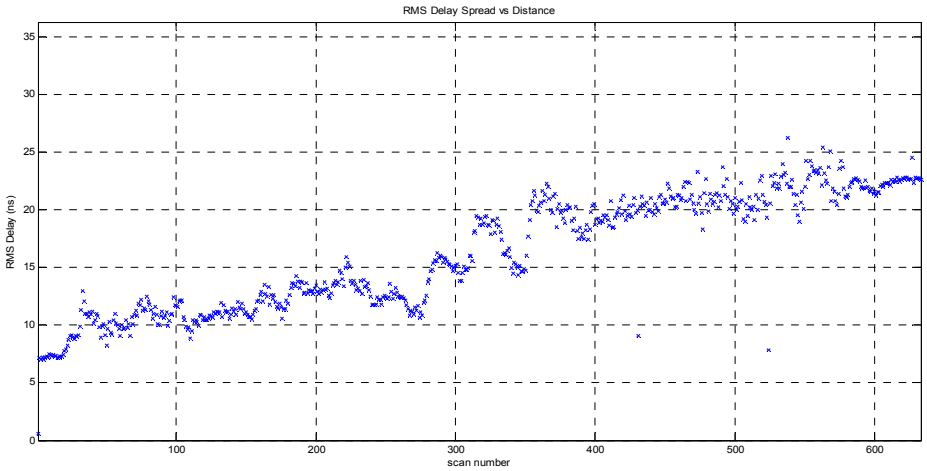

Figure 5-43 RMSDS for 5.3.2

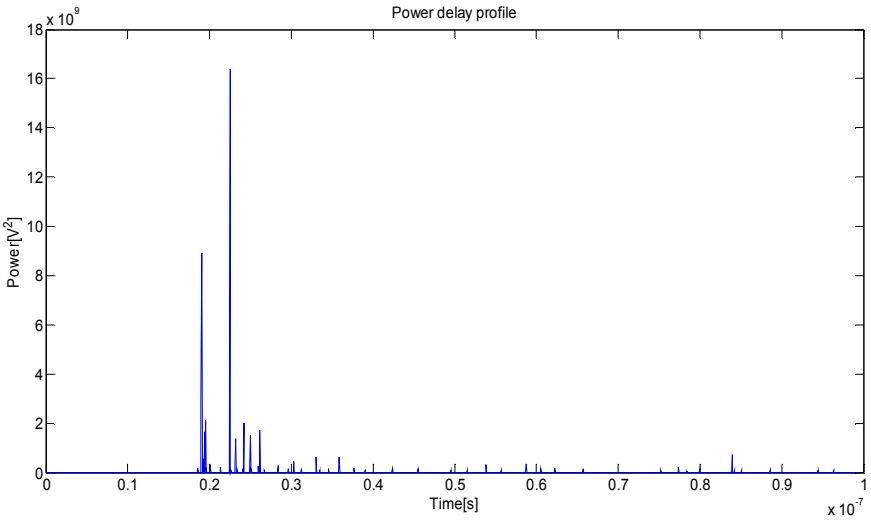

Figure 5-44 PDP for 5.3.2

Average RMS delay spread = 16.1977 ns

Maximum RMS delay spread = 26.2914 ns

Minimum RMS delay spread = 0.5692 ns

Mean_Excess_delay = 12.2504 ns

Chapter 6

CONCLUSION AND FUTURE WORK

6.1 Conclusion

- UWB signals due to high frequency resolution, can penetrate through the Gypsum wall easily than the normal brick wall.
- Here the path loss exponent (n) is measured for different wall corridor and through the wall scenarios.
- Path loss is found to be best fit by generalized extreme value distribution due to its higher log likelihood value as compared to the normal distribution proposed by IEEE 802.15.3a standard.
- Path loss exponent is found to vary from 1.1 dB ~ 1.4 dB for LOS and 2.1 dB ~ 2.6 dB for NLOS (Gypsum wall) which is better compared to IEEE.802.3a [12] for the frequency ranges up to 10 GHz.
- The statistical analysis and modeling for the time-varying RMS delay spread based on UWB channel measurement has been achieved.
- The RMSDS for LOS varies from 8 ~ 17 ns which is better than 8 ~ 12 ns quoted from IEEE.802.3a standard.
- RMSDS for through the walls scenario (NLOS) range from 20 ~ 22 ns which also is better than 14 ~ 19 ns from IEEE.802.3a standard.
- The RMSDS values shows that they increase with the distance & higher values for NLOS compared to LOS scenarios.
- RMSDS values are higher in Gypsum wall corridor than in normal brick wall corridor environment.

Table 6-1 Concludes the RMS delay spread values for various scenarios

SL No.	Type of Environment	Mean excess Delay (ns)	RMS DS (Avg.)(ns)	RMS DS (Max.)(ns)
1.	Away from RX (Brick wall corridor – LOS)	8.1805	11.4657	22.3598
2.	Towards RX (Brick wall corridor – LOS)	5.2655	8.3689	13.3266
3.	Away from RX (Gypsum wall corridor – LOS)	9.4631	16.3544	26.7763
4.	Towards RX (Gypsum wall corridor – LOS)	10.1810	17.0580	25.9434
5.	Through the wall (Classroom environment – NLOS)	19.2827	20.3215	31.1447
6.	Through TWO walls (Classroom environment – NLOS)	21.0235	22.2009	27.5065

Table 6-2 Best distributions fits for RMS delay spread for various scenarios

SL No.	Type of Environment	1st Best Fit	2nd Best Fit
1.	Away from RX (Brick wall corridor – LOS)	LOG-LOGISTIC	GEV
2.	Towards RX (Brick wall corridor – LOS)	NORMAL	RICIAN
3.	Away from RX (Gypsum wall corridor – LOS)	T LOCATION-SCALE	LOGISTIC
4.	Towards RX (Gypsum wall corridor – LOS)	WEIBULL	NORMAL
5.	Through the wall (Classroom environment – NLOS)	T LOCATION-SCALE	LOGISTIC
6.	Through TWO walls (Classroom environment – NLOS)	T LOCATION-SCALE	LOGISTIC

6.2 Future work

The analysis carried out in this thesis was performed in different indoor environments and was only limited to Gypsum wall scenario. It remains to be seen what would be the effect in the case of walls with other material. Also, the experiment can extend to different scenarios like through the floor and ceiling and see whether there are any significant changes in the penetration capacity of UWB signals. This thesis does not include the inverse scattering effects and dielectric properties of the materials used in the wall, even these topics should also be explored. As there is increase in demand on wireless infrastructure in today's world and with this statistical analysis results in hand, University can think on betterment of the existing wireless communication system in future.

Appendix A

Distribution Fits

Distribution Fits:

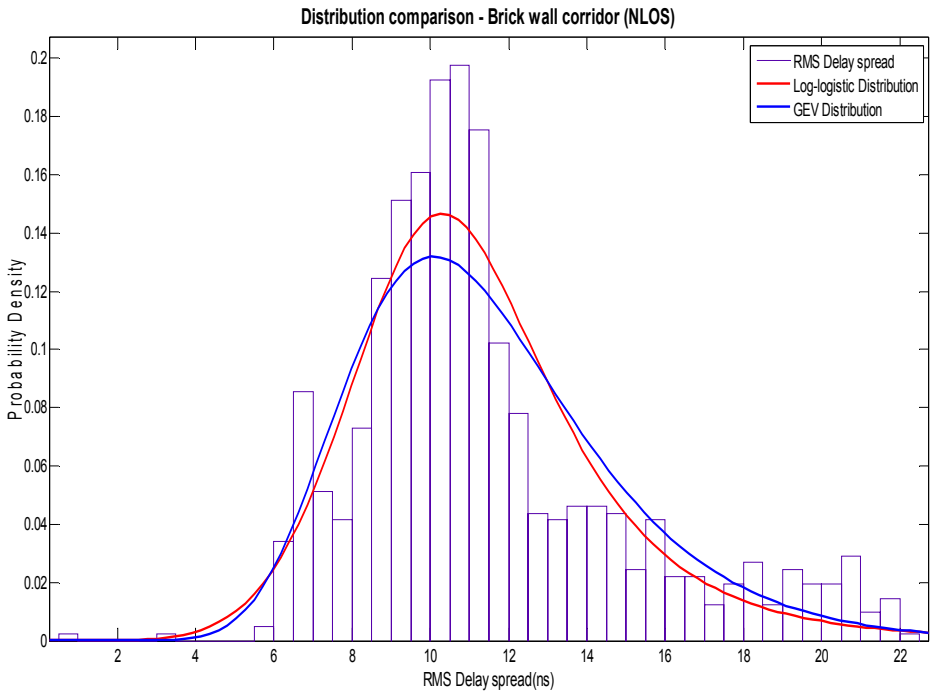

Figure A-1 RMSDS for 5.1.1

Table A-1 Comparison between distributions (for 5.1.1)

	Log-Logistic	GEV
Log likelihood	-2111.96	-2116.07
Mean	11.3346	11.4706
variance	12.2366	11.5918

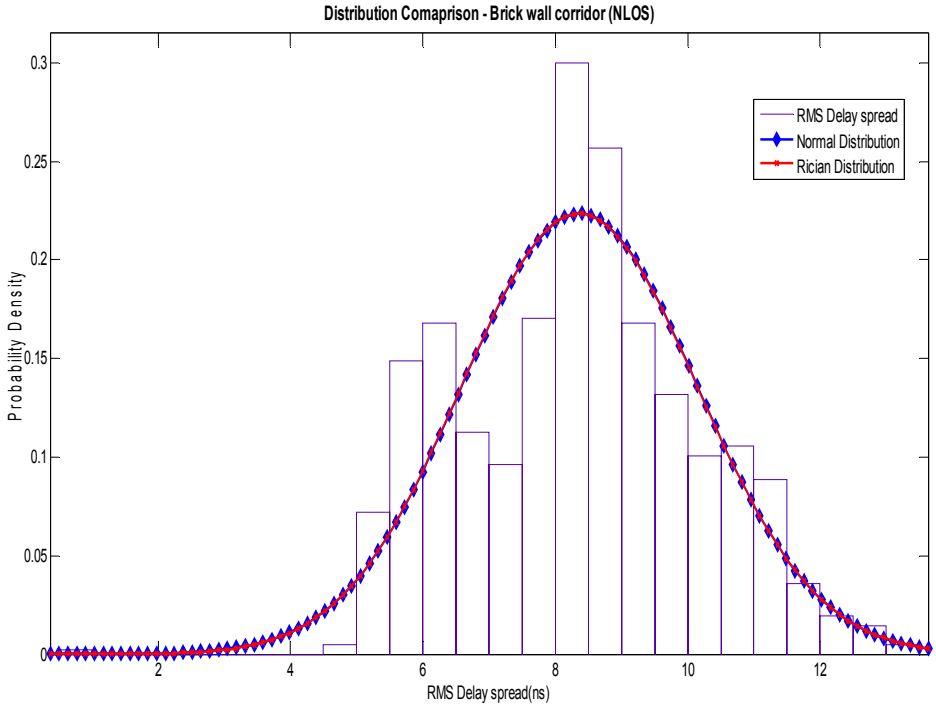

Figure A-2 RMSDS for 5.1.2

Table A-2 Comparison between distributions (for 5.1.2)

	Normal	Rician
Log likelihood	-1665.8	-1665.91
Mean	8.36885	8.36883
variance	3.18373	3.18032

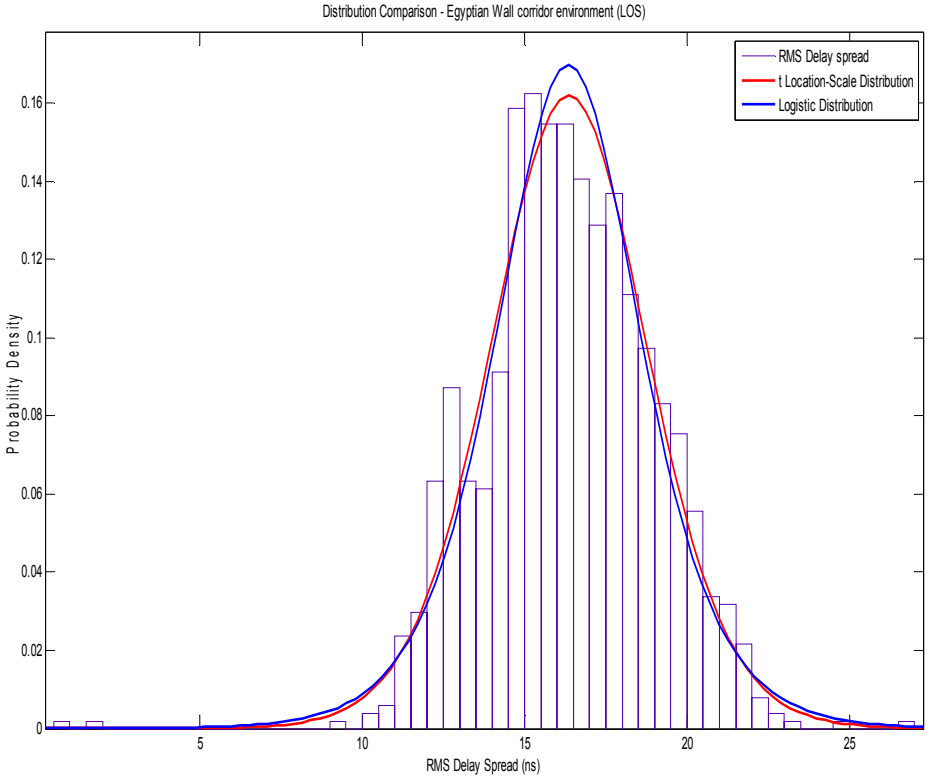

Figure A-3 RMSDS for 5.2.1

Table A-3 Comparison between distributions (for 5.2.1)

	T-Location scale	Logistic
Log likelihood	-2388.22	-2395.34
Mean	16.3592	16.3484
variance	6.70046	7.12583

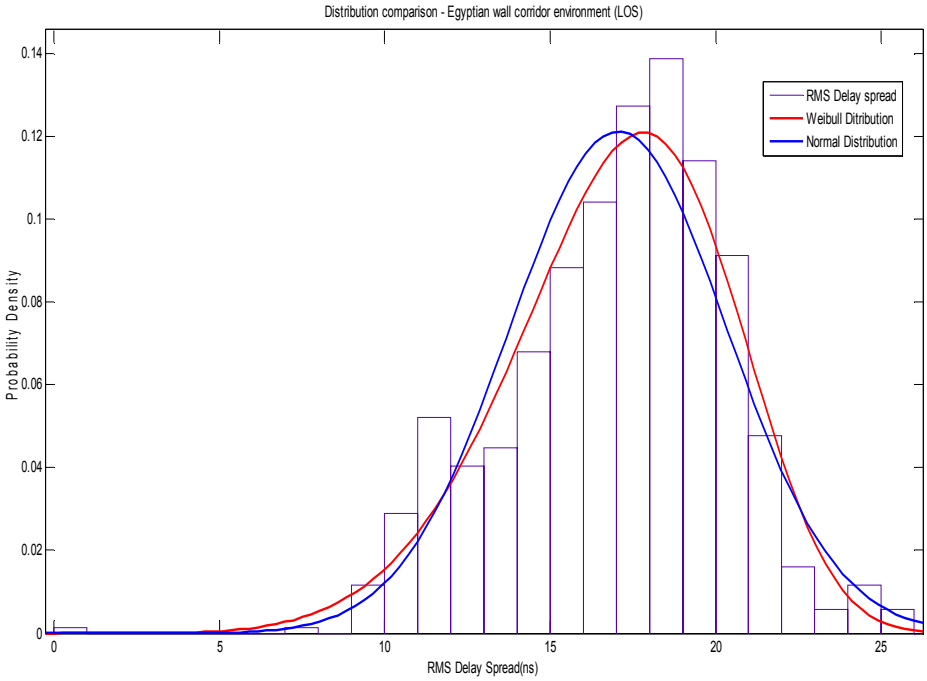

Figure A-4 RMSDS for 5.2.2

Table A-4 Comparison between distributions (for 5.2.2)

	Weibull	Normal
Log likelihood	-1801.01	-1802.5
Mean	17.0324	17.058
variance	11.0446	10.8119

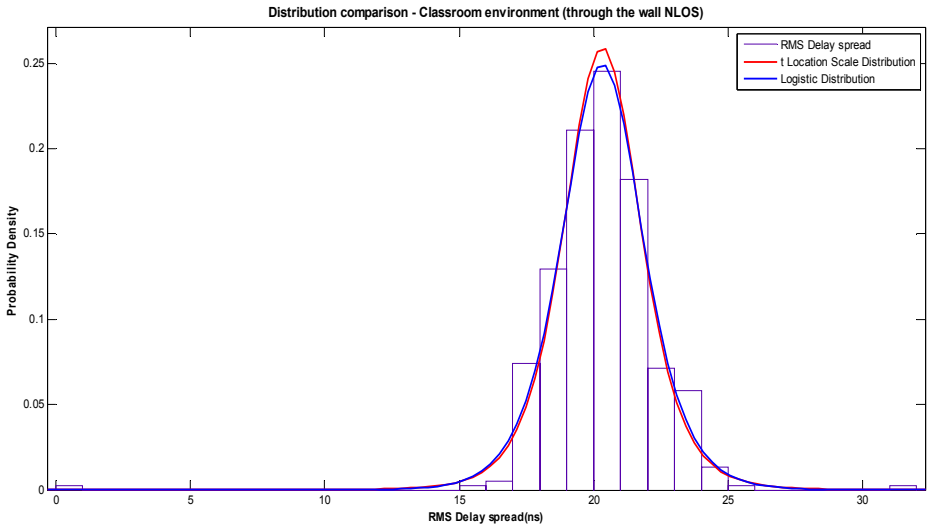

Figure A-5 RMSDS for 5.3.1

Table A-5 Comparison between distributions (for 5.3.1)

	T-Location Scale	Logistic
Log likelihood	-754.253	-761.159
Mean	20.3181	20.3215
variance	3.36735	3.2936

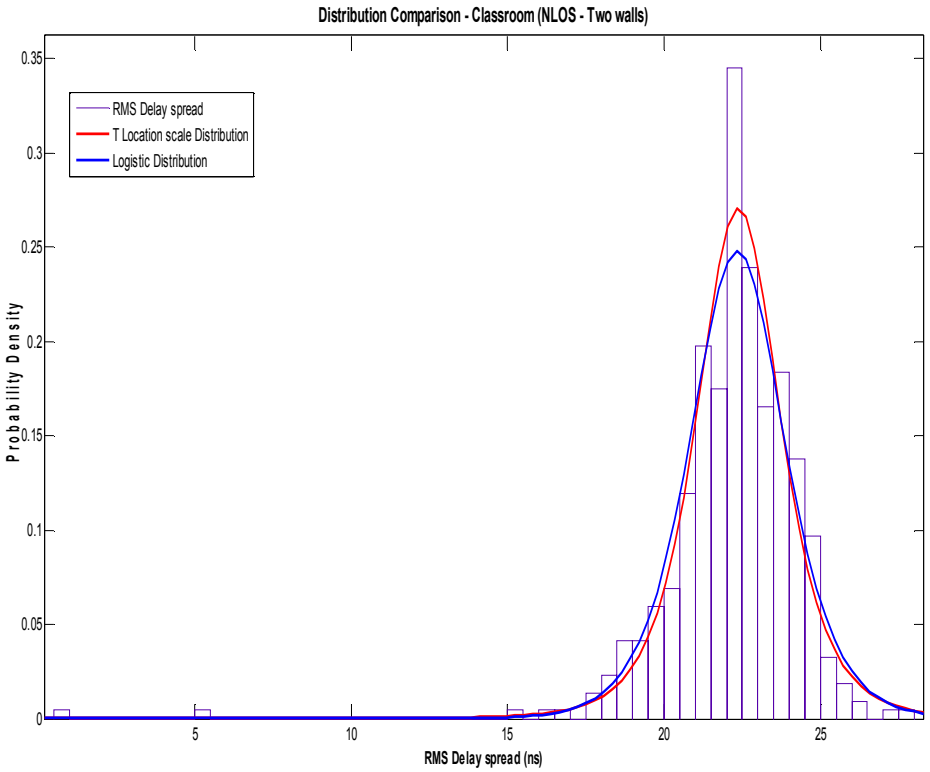

Figure A-6 RMSDS for 5.3.2

Table A-6 Comparison between distributions (for 5.3.2)

	T-Location Scale	Logistic
Log likelihood	-868.931	-882.849
Mean	22.3776	22.3411
variance	3.68505	3.35683

References

[1] Z. Irahhauten, H. Nikookar and G. Janssen, “An Overview of Modeling of Ultra Wide Band Indoor Channels”, Feb 2002

[2] Jeffrey R. Foerster, Marcus Pendergrass, and Andreas F. Molisch, “A Channel Model for Ultrawideband Indoor Communication”, March 2003

[3] Jeffrey H. Reed, “An introduction to Ultra Wideband Communications Systems”, 2005 Pearson Education, Inc., 2005

[4] Maria-Gabriella Di Benedetto – Guerino Giancola, “Understanding Ultra Wideband – Radio Fundamentals”, Pearson Education, Inc., 2004

[5] Scott M.Yano, Time Domain Corporation, “Investigating the Ultra-Wideband Indoor Wireless Channel”., 2005

[6] S.S. Ghassemzadeh, L.J. Greenstein, A. Kavcic, T. Sveinsson3, V. Tarokh, “UWB Indoor Path Loss Model for Residential and Commercial Buildings”., 2006

[7] A.A. Saleh, R.A. Valenzuela, “A statistical model for indoor multipath propagation”, IEEE J. Sel... Areas Communication 5:128-137, Feb. 1987.

[8] H. Hashemi, “The indoor propagation channel”, Proc. of the IEEE, 81:943-968, July, 1993

[9] “UWB Channel Soundings and Models — Literature Overview”, Presented at the International Workshop on Ultra-Wideband Systems 2003 in Oulu, Finland [1], slightly updated by Ulrich Schuster, ETH Z¨urich.

[10] Time Domain Corporation, "Ranging and Communication Module (RCM), Data sheet", May 2013.

[11] Time Domain Corporation, "Monostatic Radar Module (MRM), Data sheet”, May 2013.

[12] Andreas F. Molisch, Kannan Balakrishnan, Dajana Cassioli, Chia-Chin Chong, Shahriar mami, Andrew Fort,Johan Karedal, Juergen Kunisch, Hans Schantz, Ulrich Schuster, Kai Siwiak, “IEEE 802.15.4a channel model - final report”, November 2004 (San Antonio).

[13] Narges NOORI, Roghieh KARIMZADEH-BAEE, Ali ABOLGHASEMI, “An Empirical Ultra Wideband Channel Model for Indoor Laboratory Environments”., 2007

[14] Saeed S. Ghassenizadeh, Rittwik Jam Christopher W Rice, William Turin, Vahid Tarokh, “A STATISTICAL PATH LOSS MODEL FOR IN-HOME UWB CHANNELS”

[15] Yingzhi Chen, “Experimental Characterization of an Ultra-Wideband Indoor Wireless Channel”, Thesis report., 2009

[16] Monchai Chamchoy, Worawoot Doungdeun, and Sathapom Promwong, “Measurement and Modeling ofUWB Path Loss for Single-Band and Multi-Band Propagation Channel”., 2010

[17] Aawatif Menouni Hayar* and Giorgio M. Vitetta, “Channel Models for Ultra-Wideband Communications: an Overview”., 2006

[18] Ashith Kuamar,”Experimental study of through the wall human being detection using UWB radar”, Thesis report., 2011

[19] Leonard E. Miller, "Why UWB? A Review of Ultra wideband Technology," NETEX Project Office, DARPA, April 2003.

Biographical Information

Sreevinay Netrapala was born in Tumkur, India in 1989. He completed his Bachelor's in Electronics & Communications Engineering from the Visvesvaraya Technological university, India in 2011.

He worked at Infosys Technologies Ltd, India as a Software Engineer for two years prior joining the University of Texas at Arlington, to pursue his Masters in Electrical Eengineering. Sreevinay worked as Test Engineering Intern on-site at Qualcomm Inc., for six months, with Modem Power Target testing group. His research interests lies in various aspects of Wireless Communications and Embedded systems.